People's Democratic Republic of Algeria
Ministry of Higher Education and Scientific Research

University M'Hamed BOUGARA – Boumerdes

Institute of Electrical and Electronic Engineering

Department of Electronics

Final Year Project Report Presented in Partial Fulfilment of the Requirementsfor the Degree of

MASTER

In **Electrical and Electronic Engineering**

Option: **Telecommunications**

Title:

Ultra Large Band Printed Monopole Antenna

Presented by:

- **SETTOU Noureddine**
- **ZOUARI FERHAT Hamza**

Supervisor:

Mr. DEHMAS Mokrane

Registration Number:...../2016

Acknowledgements

We would like to start by thanking ALLAH, without his graciousness the completion of this work would not have been possible. We would like to thank our supervisor, ***Mr. Dehmas****, and* ***Pr. Azrar*** *as well for their continuous encouragement, invaluable supervision, timely suggestions and inspired guidance throughout the completion of this thesis.*

We would like to express our deep thanks and gratitude to ***Ms. Mouhouche*** *for her support and constant guidance through this project.*

Finally, we extend our gratitude to our beloved friend ***B. Djaafar*** *and all who are directly or indirectly involved in the successful completion of this thesis.*

Dedication

We dedicate this modest work to our parents for their love and support, this project would not have been possible without them.

And to our beloved families and friends for their words of encouragement and valuable assistance throughout our study.

Hamza

Dedication

I dedicate this thesis to my parents and

Brothers and sisters for their support, encouragement, and

understanding throughout the period of the work.

And all my friends

noureddine

Table of Contents

List of figures

Chapter 1: Generalities on Microstrip Patch Antennas

Chapter 2: Analysis of Monopole Printed Circular Antenna

Chapter 3: Ultra Large Band Printed Monopole Antenna

List of Tables

List of Acronyms

UWB: Ultra Wideband

CST: Computer Simulation Technology

MSPA: Microstrip Patch Antenna

VSWR: Voltage Standing Wave Ratio

%BW: Percent Bandwidth.

R_L: Return Loss.

D: Directivity.

FCC: Federal Communications Commission

FBW:fractional bandwidth

LB: Large Band

ULB: UltraLarge Band

PCMA: Printed Circular Monopole Antenna

WLAN: Wireless local area network

WIMAX: Worldwide interoperability for microwave access.

ABSTRACT

In this work, an Ultra Large Band modified circular shape printed monopole antenna operating in the frequency range extending from 2.60 GHz to 12.15 GHz has been developed.

This is achieved by first introducing to the considered original circular shaped antenna defects that resulted in a simulated ULB behavior. The obtained monopole structure has been fabricated and its reflection coefficient measured. A good agreement is observed with the simulated results. The measured antenna percent bandwidth is 129 % whereas the simulated one is 149%. In addition, the antenna simulated and measured refection coefficients present a quite similar form over the frequency range where a good impedance matching is observed.

The antenna can operate in different frequency bands (S, C and X) and hence, it is suitable for the various applications covered by these bands.

Moreover, different radio electric properties including input impedance, current distribution as well as 2D and 3D radiation patterns are simulated using the CST Microwave Studio tool.

Introduction

In nowadays, wireless communication has become a part of human life and with the rapid development of modern communication and semiconductor technologies [1], a wide variety of wireless services have been successfully introduced worldwide [2]. Most of the electrical and electronics equipment around us are using the wireless communication systems. From mobile telephones to wireless Internet access to networked appliances and peripherals, there is an increasing dependence on wireless communications to provide functionality for products and services. Technologies of wireless communication systems always need further improvement to satisfy higher resolution and data requirements; the Antenna is a very essential component of the system.

Antenna is an electrical device which transmits the electromagnetic waves into the space by converting the electric power given at the input into the radio waves and at the receiver side the antenna intercepts these radio waves and converts them back into the electrical power. It is used in systems such as radio broadcasting, broadcast television, two-way radio, communications receivers, radar, cell phones, and satellite communications, as well as other devices such as garage door openers, wireless microphones, Bluetooth-enabled devices, wireless computer networks and baby monitors. So, modern and future wireless communication systems are placing a greater demand on the antenna designs to cover several operating frequency bands of wireless communication systems and having high gain, small physical size, versatility and stability. The demands of smart antenna design for more reliable mobile communication systems have been increased day by day. Recently, ultra-wideband “UWB” has become a very promising wireless technology for any applications because of the attractive benefits it provides such as its resistance against jamming and multipath fading, low complexity and cost, power requirements and finally penetrating capability. According to the FCC the spectral mask of UWB for commercial applications is of frequency band 3.1 to 10.6 GHz [3]. The design of UWB antennas has received much attention in the research community. In recent years, most of these designs use canonical elements such as circles or ellipses as radiating element. Combinations of these elements have also been used [4]. Monopole printed antennas are good candidates for such systems because of their numerous advantages such as small size, lightweight, low profile, low

cast and ease of integration with other microwave components. It is being used in large variety of applications such as radar, missiles, aircraft, satellite communications, mobile communication base stations, handsets as well as in biomedical telemetry services [5]. However, printed patch antennas also have some limitations with respect to conventional microwave antennas such as narrow bandwidth and relatively poor radiation efficiency resulting from surface wave excitation, conductor and dielectric losses as well as difficulty of prediction of the performances of these forms of radiator.

This project deals with development and analysis of a printed monopole patch antenna using High Frequency Structure Simulator (CST) to find a structure with a large frequency band and acceptable input impedance to avoid matching problems. The final structure is fabricated and its reflection coefficient measured.

This report includes three main chapters and it is organized as follows:

Chapter one presents overview on microstrip patch antennas including a general description, feeding techniques, advantages/disadvantages, applications as well as the method of analysis of these antennas and the difference between the printed and microstrip aspects.

Chapter two deals with an overview about the monopole printed antennas and the analysis of a proposed monopole circular shape printed antenna simulation results (return loss, VSWR, radiation patterns, etc.).

Chapter three deals with the development of a new Ultra Large band printed monopole antenna which has been fabricated. It presents an analysis of the proposed antenna as well as the measured characteristics.

Chapter One

Generalities on Microstrip Patch Antennas

1.1 Introduction

In its most fundamental form, a microstrip patch antenna consists of a radiating patch on one side of a dielectric substrate which has a ground plane on the other side. The radiating patch and the feed lines are usually photo etched on the dielectric substrate. Microstrip patch antennas radiate primarily because of the fringing fields between the Patch edge and the ground plane. For good antenna performance, a thick dielectric substrate having a low dielectric constant is desirable since this provides better efficiency, larger bandwidth and better radiation. Microstrip patch antennas are increasing popularity for use in wireless applications due to their low-profile structure. Therefore, they are extremely compatible for embedded antennas in handheld wireless devices such as cellular phones, pagers etc. [6].

1.2 Microstrip Antenna Geometry and Construction

A microstrip antenna is a resonant style radiator. It consists of a radiating patch on one side of a dielectric substrate with a ground plane on the other side. Generally, the patch consists of a conducting material such as copper which is the source of radiation where electromagnetic energy fringes off the edges of the patch and into the substrate. The length L of the patch is usually $0.333\ \lambda_0 \leq L \leq 0.5\ \lambda_0$ (λ_0 is the free space wavelength). The patch is selected to be very thin such that $t << \lambda_0$ (t is the patch thickness).

The ground plane acts as a perfectly reflecting plane bouncing energy back through the substrate and into free space. The patch and the ground plane are separated by a dielectric sheet (referred to as the substrate). There are numerous substrates materials that can be used for the design of microstrip antennas and their dielectric constant is usually in the range $2.2 \leq \varepsilon r \leq 12$ suitable for operation at frequencies ranging from 1 to 100 GHz. The ones that are most desirable for antenna performance are thick substrates whose dielectric is in the lower end of the range because they provide better efficiency and larger bandwidth [7].

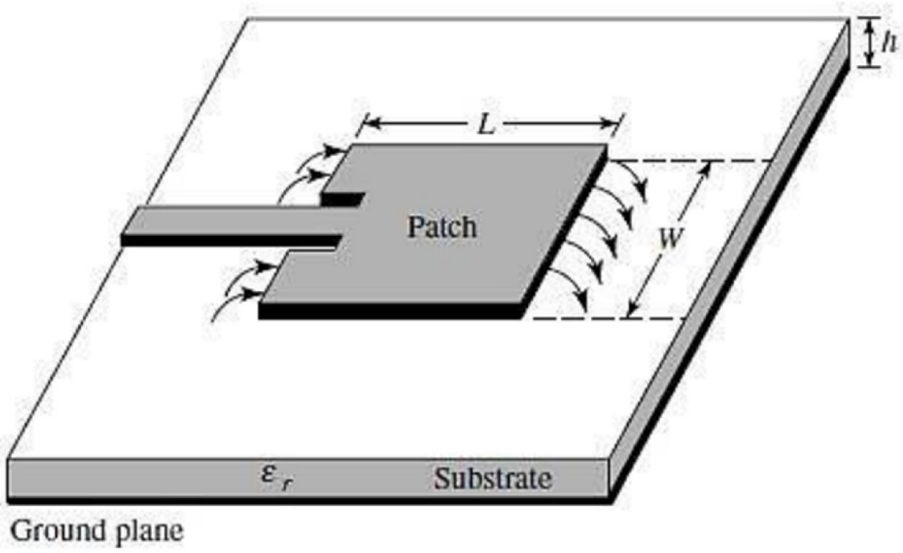

Figure 1.1 Microstrip Patch Antenna.

1.3 Types of microstrip antennas

The general form of a microstrip antenna consists of a patch of metal deposited on top of a grounded substrate. The patch can be rectangular, circular, square, triangular or any other shape as shown in figure 1.2 [8]. Rectangular and circular are the most commonly used shapes mainly because to their simplicity and fabrication ease.

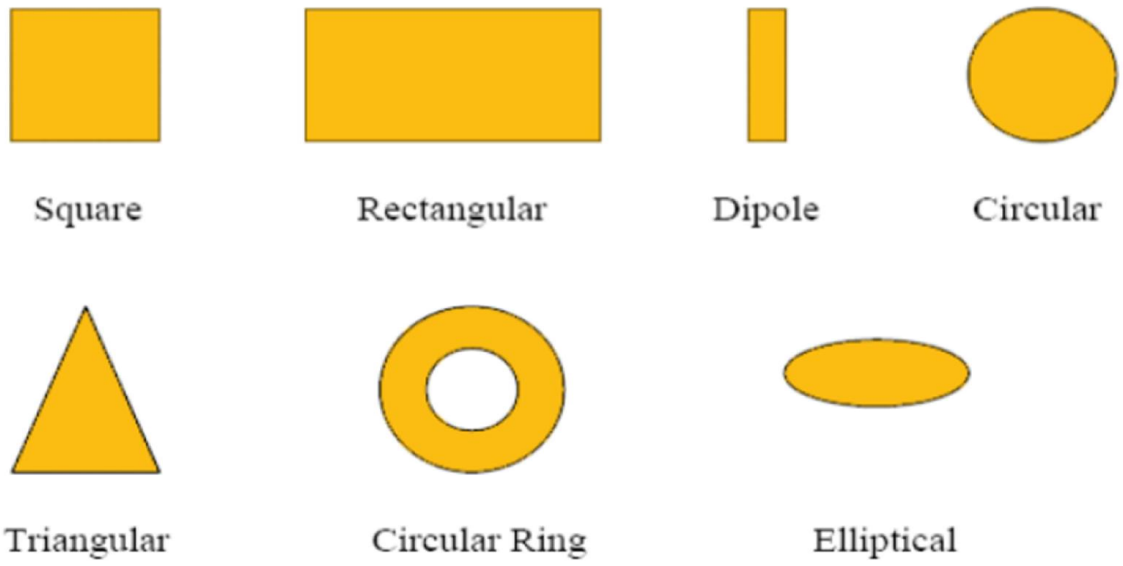

Figure 1.2 Different Shapes of Microstrip Antennas [8].

1.4 Radiation mechanism

To understand the mechanism behind the radiation from microstrip antenna considers a rectangular antenna with a half wavelength long radiating patch fed by microstrip feed line. A rectangular antenna can be considered as a microstrip line left open ended on one side and energy is fed from the other end. Since the patch is half wavelength long and left open ended on other side, the current at the corners (at the beginning and end) of the patch should be zero and is maximum at the center of the patch. Current and voltage will be 90 degrees out of phase. The voltage will be maximum positive at the beginning and maximum negative at the end of patch [10].

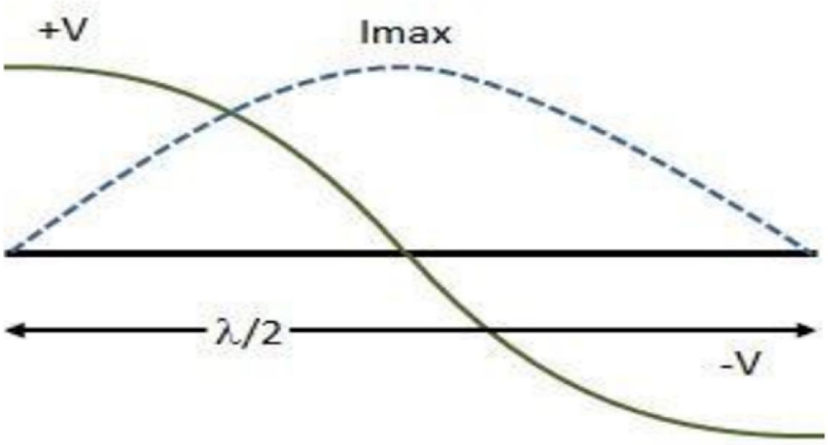

Figure 1.3 Current and voltage variation along the Patch length.

Field distribution along the patch is like shown in figure 1.4. The field lines are below the patch towards corner are opposite in direction. This field lines do not stop abruptly ant the end. At the corners, fringing fields are created and the field lines are in bow shape. More the fringing field bow more the radiation. Therefore, these fringing are the reason behind the radiation from the microstrip antenna.

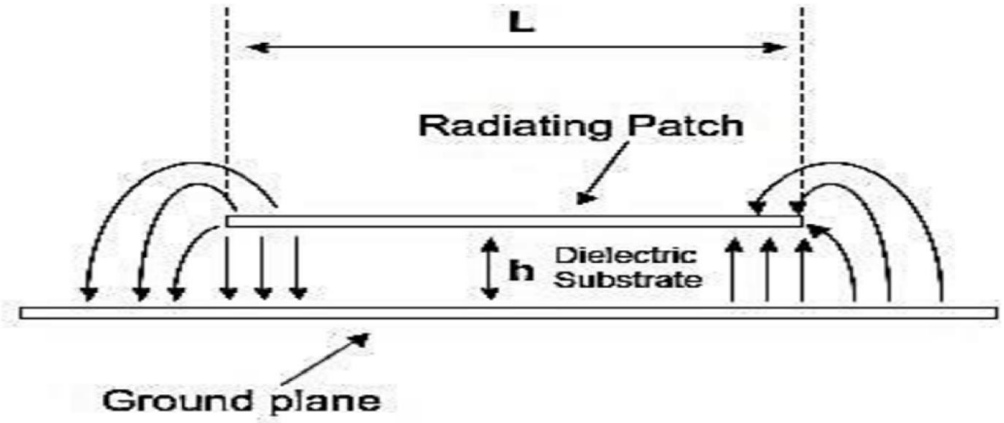

Figure1.4 Fringing fields [7].

1.5 Feed techniques

Microstrip patch antennas can be fed by a variety of methods. These methods can be classified into two categories*: **contacting and non-contacting.***

In the contacting method, the RF power is fed directly to the radiating patch using a connecting element such as a microstrip line. In the non-contacting scheme, electromagnetic field coupling is done to transfer power between the microstrip line and the radiating patch. The four most popular feed techniques used are the microstrip line, coaxial probe (both contacting schemes), aperture coupling and proximity coupling (both non-contacting schemes).

1.5.1 Microstrip line feed

In this type of feed technique, a conducting strip is connected directly to the edge of the Microstrip patch as shown in Figure 1.5. The conducting strip is smaller in width as compared to the patch and this kind of feed arrangement has the advantage that the feed can be etched on the same substrate to provide a planar structure.

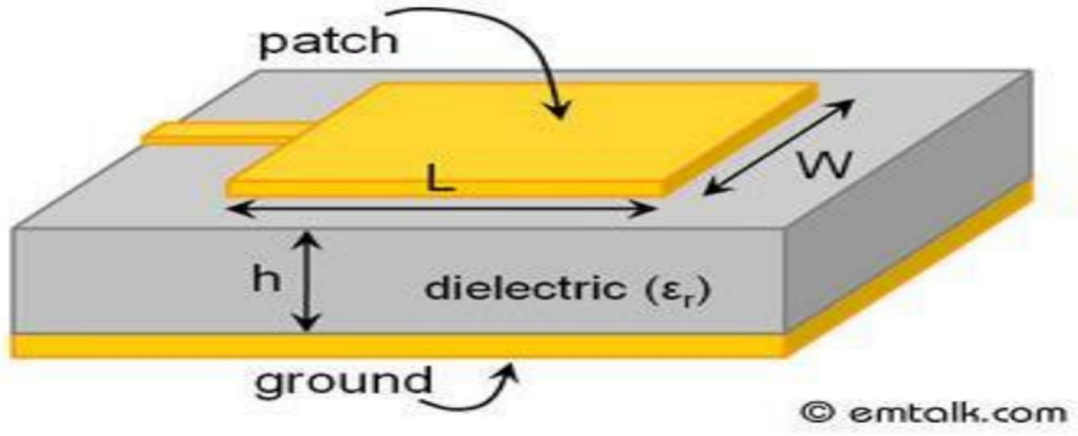

Figure 1.5 Microstrip line feed.

The purpose of the inset cut in the patch is to match the impedance of the feed line to the patch without the need for any additional matching element. This is achieved by properly controlling the inset position. Hence this is an easy feeding scheme, since it provides ease of fabrication and simplicity in modeling as well as impedance matching. However, as the thickness of the dielectric substrate being used, increases, surface waves and spurious feed radiation also increases, which hampers the bandwidth of the antenna. The feed radiation also leads to undesired cross polarized radiation.

1.5.2 Coaxial feed

The Coaxial feed or probe feed is a very common technique used for feeding Microstrip patch antennas. As seen in figure 1.6, the inner conductor of the coaxial connector extends through the dielectric and is soldered to the radiating patch, while the outer conductor is connected to the ground plane.

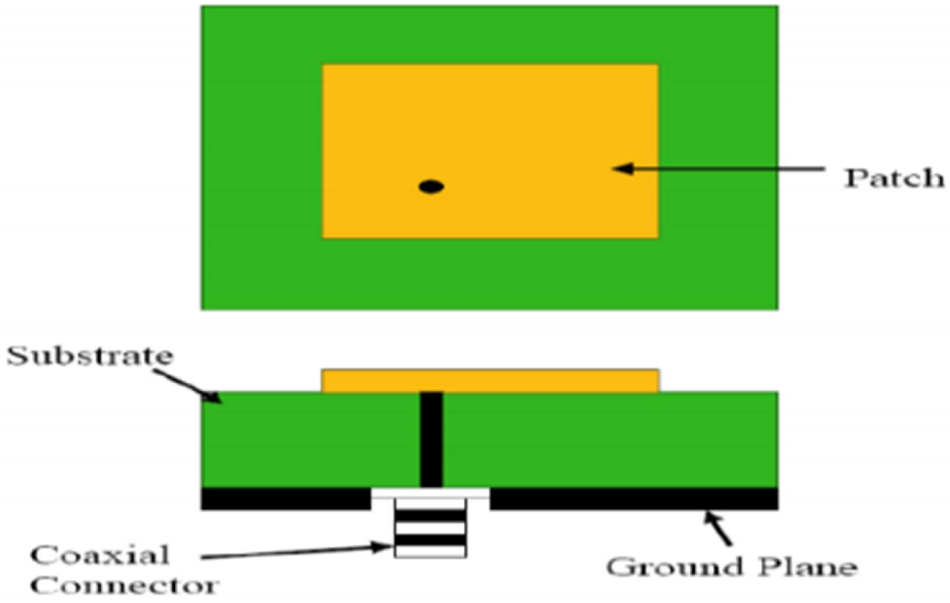

Figure1.6 Probe fed Rectangular Microstrip Patch Antenna.

The main advantage of this type of feeding scheme is that the feed can be placed at any desired location inside the patch in order to match with its input impedance. This feed method is easy to fabricate and has low spurious radiation. However, a major disadvantage is that it provides arrow bandwidth and is difficult to model since a hole has to be drilled in the substrate and the connector protrudes outside the ground plane, thus not making it

completely planar for thick substrates (h >0.02λo). Also, for thicker substrates, the increased probe length makes the input impedance more inductive, leading to matching problems [11]. It is seen above that for a thick dielectric substrate, which provides broad bandwidth, the microstrip line feed and the coaxial feed suffer from numerous disadvantages. The non-contacting feed techniques which have been discussed below, solve these issues.

1.5.3 Aperture coupled feed

In this type of feed technique, the radiating patch and the microstrip feed line is separated by the ground plane as shown in Figure 1.7. Coupling between the patch and the feed line is made through a slot or an aperture in the ground plane.

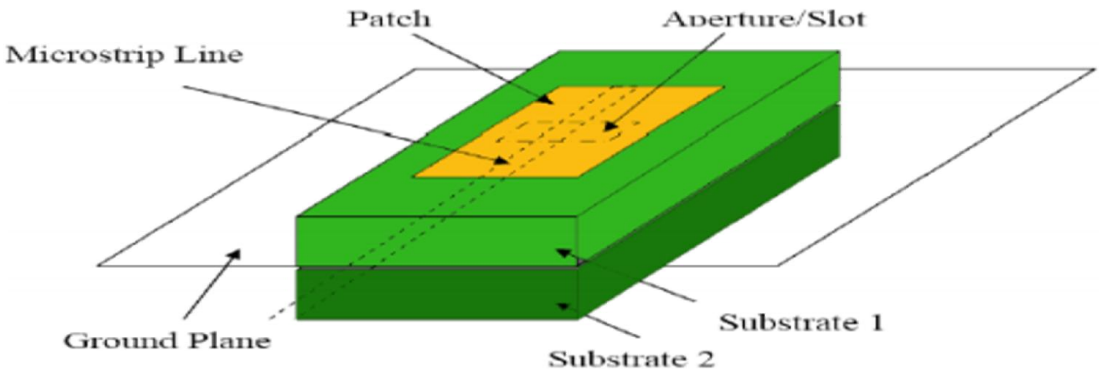

Figure 1.7 Aperture coupled feed [12].

The coupling aperture is usually centered under the patch, leading to lower cross-polarization due to symmetry of the configuration. The amount of coupling from the feed line to the patch is determined by the shape, size and location of the aperture. Since the ground plane separates the patch and the feed line, spurious radiation is minimized. Generally, a high dielectric material is used for bottom substrate and a thick, low dielectric constant material is used for the top substrate to optimize radiation from the patch. The major disadvantage of this feed technique is that it is difficult to fabricate due to multiple layers, which also increases the antenna thickness. This feeding scheme also provides narrow bandwidth.

1.5.4 proximity coupling

This type of feed technique is also called as the electromagnetic coupling Scheme. As shown in figure 1.8, two dielectric substrates are used such that the feed line is between the two substrates and the radiating patch is on top of the upper substrate. The main advantage of this feed technique is that it eliminates spurious feed radiation and provides very high bandwidth.

Due to overall increase in the thickness of the microstrip patch antenna. This scheme also provides choices between two different dielectric media, one for the patch and one for the feed line.

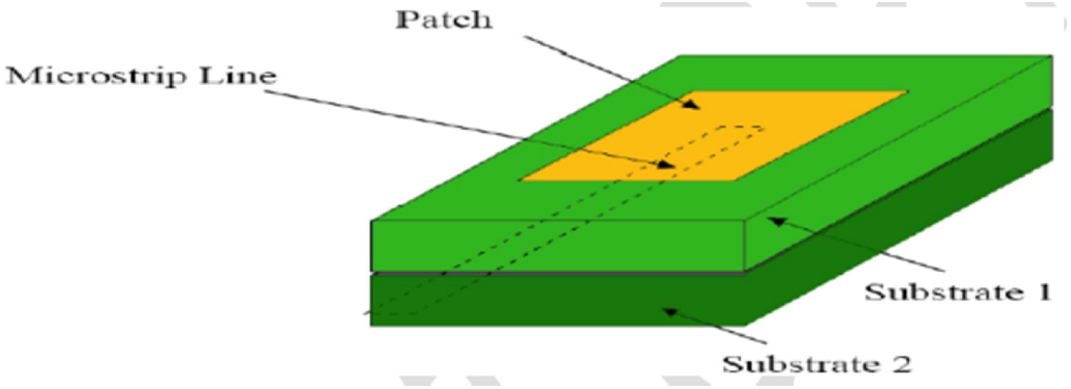

Figure 1.8 Proximity Feed Technique [13].

1.6 Analysis Methods of Microstrip Antenna

There are many methods for microstrip antenna analysis. The most popular are transmission line model (in which we assume that the patch is a transmission line or a part of a transmission). The second is the cavity model (here we assume that the patch is a dielectric-loaded cavity) and the third method is the full wave model or analysis.

1.6.1TransmionLinemodel

The transmission line model treated rectangular microstrip as a part of transmission line. As the rectangular microstrip antenna consists of two radiating edges, transmission line model represents each radiating edge by an equivalent admittance which is separated by a distance equal to the length. The resistive part of them represents the radiation loss from each edge. At the resonance, the reactive part of the input impedance cancelled out and the input impedance become pure resistive [7].

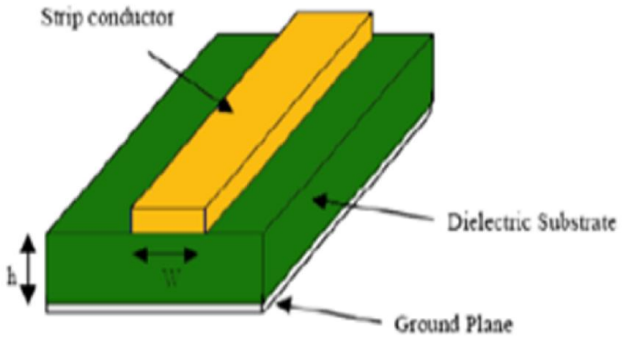

Figure 1.9 Microstrip line.

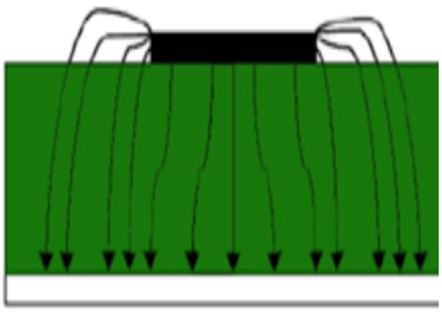

Figure 1.10 Electric field lines [13].

1.6.2 Cavity Model

The cavity model is based on the assumption that the region between the microstrip patch and ground plane is a resonant cavity bounded by ceiling and floor of electric conductors and the magnetic walls along the edge of the conductor as shown in figure 1.11 [11-14-15].

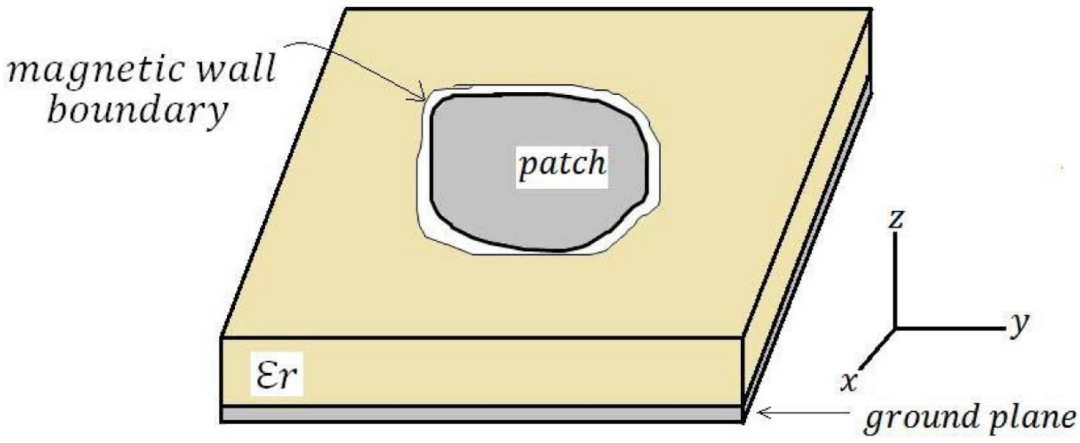

Figure 1.11 Magnetic wall model of microstrip patch antenna.

1.6.3 Full Wave Model

This model includes primarily integral equations and Moment Methods. It is extremely accurate, versatile and can treat single elements, finite and infinite arrays, stacked elements, arbitrary shaped elements and coupling. This model gives less insight as compared to the two models mentioned above and is far more complex in nature.

1.7 Microstrip Antenna Parameters

An antenna is an electrical conductor or system of conductors. The IEEE definition of an antenna as given by Stutzman and Thiele is "That part of a transmitting or receiving system that is designed to radiate or receive electromagnetic waves" [16]. The major parameters associated with an antenna are defined in the following sections.

1.7.1 Input Impedance

The input impedance of an antenna is defined as "the impedance presented by an antenna at its terminals or the ratio of the voltage to the current at the pair of terminals or ratio of the appropriate components of the electric to magnetic fields at a point" Hence the impedance of the antenna can be written as:

$$Z_{in} = R_{in} + j\,X_{in} \qquad (1.1)$$

Where,

$\mathbf{Z_{in}}$ is the antenna input impedance

$\mathbf{R_{in}}$ the input resistance

$\mathbf{X_{in}}$ the input reactance

1.7.2 Return Loss

Return loss is an important parameter when testing an antenna. It is related to impedance matching and the maximum transfer of power theory. It is also a measure of the effectiveness of an antenna to deliver of power from source to antenna. The return loss (R_L) is defined by the ratio of the power reflected back from the antenna P_{ref} to the source incident power of the antenna P_i. Its mathematical expression is:

$$\mathbf{R_{LdB}= 10 \log \left(\frac{p_{ref}}{p_{in}}\right)} \qquad (1.2)$$

1.7.3 Voltage standing wave ratio (VSWR)

For an antenna to perform efficiently there is always a reflection of the power, which leads to the standing waves, which is characterized by the voltage standing wave ratio (VSWR).This is given by[15]:

$$\mathbf{VSWR = \frac{V_{max}}{V_{min}} = \frac{1- |\Gamma|}{1+ |\Gamma|}} \qquad (1.3)$$

Where the reflection coefficient $\boldsymbol{\Gamma}$ is given by:

$$\boldsymbol{\Gamma = \frac{Z_i - Z_o}{Z_i + Z_o}} \qquad (1.4)$$

$\mathbf{Z_i}$ is the input impedance and $\mathbf{Z_0}$ is the characteristics impedance of the feed line.

Moreover, the antenna return loss and reflection coefficient are related by the equation:

$$\mathbf{R_{L\ dB}= 20 \log_{10} I \Gamma I} \qquad (1.5)$$

1.7.4 Bandwidth

It is defined as “The range of usable frequencies within which the performance of the antenna, with respect to some characteristic, conforms to a specified standard”. Considering the

power transfer from the source to the antenna, the bandwidth is usually defined as the range of frequencies for which:

$$R_{L\,dB} \leq -10\ dB \qquad (1.6)$$

Or, using eqs. 1.3 and 1.5, it corresponds to the frequency range for which

$$1 \leq VSWR \leq 2 \qquad (1.7)$$

The percent bandwidth is expressed as:

$$BW\% = \frac{f_h - f_l}{f_c} \times 100 \qquad (1.8)$$

Where f_l and f_h denote respectively the lower and upper limit of the bandwidth and the center frequency.

1.7.5 Antenna radiation patterns

The radiation pattern is defined as "a mathematical function or a graphical representation of the radiation properties of the antenna as a function of space coordinates" [14].

Fig. 1.12 illustrates some parameters related to the antenna radiation pattern concept.

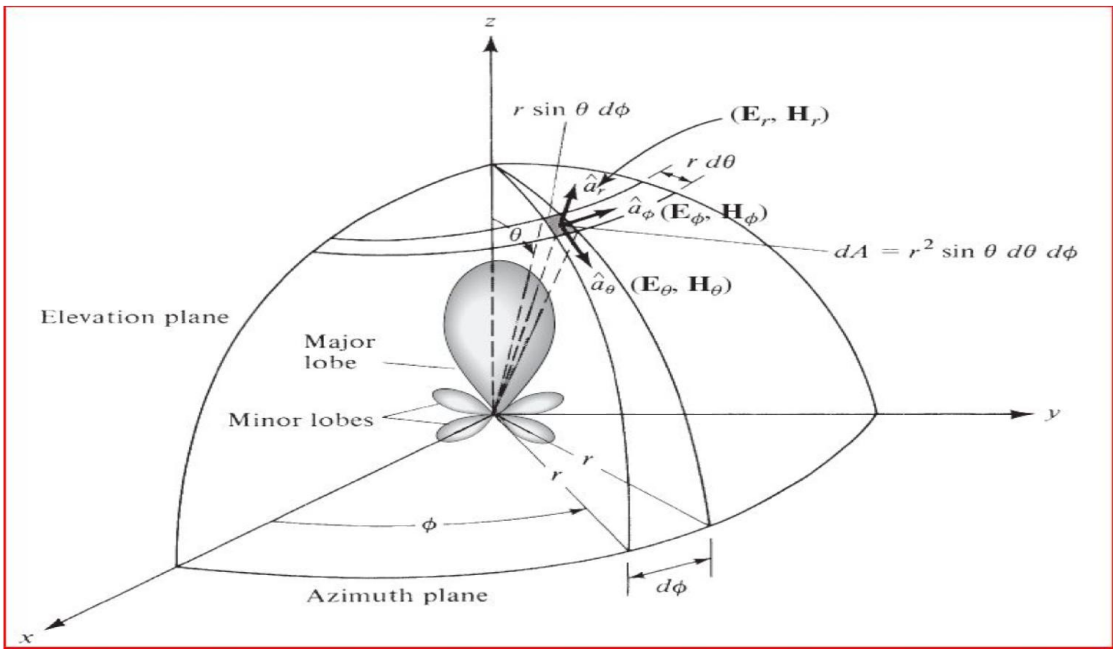

Figure 1.12 Coordinate system for antenna analysis [11].

1.7.6 Directivity

The directivity of an antenna defined as the ratio of the radiation intensity in a given direction from the antenna to the radiation intensity averaged over all directions [9].

$$\mathbf{D} = \frac{U}{U_0} = \frac{U}{P_{rad}/4\pi} = \frac{4\pi}{P_{ra}} \quad (1.9)$$

The maximum directivity is expressed as

$$D_{max} = D_0 = \frac{U_{max}}{U_0} = \frac{4\pi U_m}{P_{rad}} \quad (1.10)$$

1.8 Application

The advantages of microstrip antenna make them suitable for numerous applications:

Table 1.1 Typical Applications of Microstrip Antennas.

SYSTEM	APPLICATION
Aircraft and ship antenna	Communication and navigation, altimeter, blind landing
Missiles	Radar, proximity fuses and telemetry
Satellite communication	Domestic direct broadcast tv, vehicle-based antennas, communication
Mobile radio	Pagers and hand telephones, man pack systems, mobile vehicle
Remote sensing	Large lightweight apertures
Biomedical	Application in microwave hyperthermia

1.9 Advantages and disadvantages of microstrip antenna

Microstrip patch presents advantages and disadvantages as shown in the following table. However, some of their disadvantages, such as bandwidth limitation, can be overcome by using techniques some design.

Table 1.2 Typical Applications of Microstrip Antennas.

Advantages	**disadvantages**
Lightweight, low volume	Narrow bandwidth
Easy to mount	Loss
Low fabrication cost	Poor end-fire radiation characteristics
Aerodynamic (good for fitting on missiles and ships)	Very limited maximum gain
Linear and circular polarization easy to implement by position of feed	Poor isolation between feed and antenna
Dual frequency use possible	
Feed lines and matching fabricated with antenna	

1.10 Ultra wideband (UWB)

The first practical UWB systems are really more than 100 years old. Ultra-wideband communications started to receive renewed interest in the 1970's. At that time, it was called 'baseband' or 'carrier-free' communications. Around 1973, it was recognized the short pulses, which spread the signal over a large spectrum, which is not significantly affected by existing narrowband interferers, and do not interfere with them. UWB communications continued to be mostly investigated in the military sector, the pioneering work of Win and Scholtz showed that impulse radio could sustain a large number of users by assigning pseudorandom transmission times to the pulses from the different users. This insight, coupled with advances in electronics device design, spawned the interest of commercial wireless companies into UWB [18].

It is noteworthy that UWB antenna research never experienced the slump of UWB communications, but rather stayed a popular and important area throughout the past 70 years. A

main factor in this development was TV broadcasting: the assigned TV bands extend over a large frequency range, and since it is desirable that a single antenna can transmit and receive all available stations, it implied that the antenna had to be very broadband as well[18].

Another key obstacle to commercial use of UWB was political in nature. Frequency regulators all over the world assign narrow frequency bands to specific services and/or operators. UWB systems violate those frequency assignments, as they emit radiation over a large frequency range, including the bands that have already been assigned to other services, those type of antennas not allowed to be placed on outdoor structures. The potential interference depends on when and where the device is used, its transmission power level, numbers of device operating, pulse repetition frequency, direction of the transmitted signal, etc. [19]. Proponents of UWB tried to convince the frequency regulator in the USA, the FCC (Federal Communications Commission), that the emissions from UWB devices would not interfere with those other services. After a lengthy hearing process, the FCC issued a ruling in 2002 that allowed intentional UWB emissions in the frequency range between 3.1 and 10.6 GHz with fractional bandwidth measured at "−10 dB" points subjected to certain restrictions for the emission power spectrum, A UWB system is supposed to be used for a short range communication. Although the FCC has allowed UWB devices to operate under mandatory emission masks as shown in Table 2 above, testing on the interference of UWB with other wireless systems should and will still continue. Given the identified bands and failure to comply with the regulations aforementioned, UWB systems could become a potential jammer for the numerous licensed services [19], as UWB communications emerged as a commercially viable option, the development of smaller antennas became a new requirement [18].

To satisfy such requirement various wideband antennas have been studied. But some of them cannot cover the whole bandwidth. Among many possible alternatives, monopole antennas have been extensively investigated because of their attractive features such as light weight, simple structure and ease of mass production and many results have been obtained [17]

Table1.3 UWB classification

Region	UWB band
United states	**Single band: 3.1 GHz ___ 10.6 GHz**
Europe	**Low band : 3.1 GHz ____ 4.8 GHz** **High band : 6 GHz _____8.5 GHz**
japan	**Low band : 3.4 GHz_____4.8 GHz** **High band : 7.25 GHz__10.25 GHz**

1.11 UWB specifications

Bandwidth (BW) is simply the difference between the upper (fh) and lower (fl) operating frequency:

$$\boldsymbol{Bw = fh - fl} \qquad (1.11)$$

The bandwidth of a system is often described relative to the center frequency (fc). Often, the centered frequency is defined as the arithmetic average of the upper and lower operation frequencies:

$$\boldsymbol{fc = \frac{1}{2}(fh + fl)} \qquad (1.12)$$

An alternate definition of the center frequency involves the geometric average:

$$\mathbf{fc = \sqrt{fl \times fh}} \qquad (1.13)$$

The fractional bandwidth (bw) of a system is the ratio of the bandwidth to the center frequency:

$$\mathbf{bw = \frac{Bw}{fc}} \qquad (1.14)$$

The fractional bandwidth varies between 0 and 2, and is often quoted as a percentage (between 0% and 200%). The higher the percentage, the wider the bandwidth.

Using the arithmetic average definition of center frequency, the percent fractional bandwidth is given by:

$$\% \text{ BW} = 200 \frac{(fh - fl)}{(fh + fl)} \% \qquad (1.15)$$

The percent fractional bandwidth (FBW) can determine whether the antenna is classified as WB or UWB or ULB.

Wideband antennas typically have a Fractional Bandwidth of 20% to 50 %. Antennas with a FBW of greater than 50% are referred to as ultra-wide band antennas. Antennas with a FBW of greater than 120% are considered as ultra large band.

1.12 Printed Monopole antennas

Monopole antennas are widely. A conventional monopole is a straight wire vertically installed above a ground plane. It is vertically polarized and has a quite omnidirectional radiation pattern. To increase the impedance bandwidth of the monopole antenna, planar elements can be used to replace the wire elements. In its form using microstrip technology, the UWB systems can be sorted by feeding methods; microstrip feeding and coplanar waveguide feeding. There are different types of the patch shape in the microstrip fed UWB antennas such as rectangular, triangular, circular and elliptical**.**

Printed monopole antennas are widely used in the wideband communication systems. They are lightweight, low cost, compact, planar and easy to fabricate. These antennas are good candidate for hand-held UWB applications. They are popular planar antennas for wireless communications because they provide wide impedance bandwidth and omnidirectional radiation patterns. Monopole antennas are theoretically explained by considering them as modified microstrip antennas [17]. The microstrip ground plane that is placed at the back has been removed and placed with partial ground plates at the radiating patch plane to obtain the monopole printed antenna with the omnidirectional radiation properties. In some applications where the antenna is a part of a full printed microwave circuit, the ground plane is etched in the area facing the radiating element to allow radiation in that direction.

Chapter two

Analysis of Monopole printed circular antenna

In this chapter, a conventional printed circular monopole antenna PCMA fed by a 50-Ω micro-strip is analyzed and discussed using the computer simulation technology "CST" software. This structure has been considered in [20] where it has been used as a basic structure for design of [reconfigurable frequency antenna conception], by assuming some parameter values we obtained our simulation results.

2.1 Introduction

The monopole antenna was invented in 1895 by radio pioneer Guglielmo Marconi during his historic first experiments in radio communication. He began by using Hertzian dipole antennas consisting of two identical horizontal wires ending in metal plates. He found by experiment that if instead of the dipole, one side of the transmitter was connected to a wire suspended overhead, and the other side was connected to the Earth, he could transmit for longer distances. For this reason the monopole is also called a *Marconi antenna*, although Alexander Popov independently invented it at about the same time [21].

Recently, there is an increasing interesting developing a single compact terminal which can provide more than one wireless communication service. The co-planar monopole antenna has attracted the most attention since it can be integrated with other devices in the system. The ground-plane effects on planar monopole antennas are an important issue and have been investigated by some researchers [22].

In this printed co-planar monopole antenna, we are trying to generate UWB to meet the application for wireless local area network (WLAN: 2.4–2.483GHz, 5.15–5.35GHz, and 5.725–5.85 GHz), worldwide interoperability for microwave access (WIMAX: 2.5–2.69GHz and 5.25–5.85 GHz) systems. Among the UWB antenna designs in the recent literature, monopole antennas are widely employed because of their simple structure and low cost. Circular patch is the second most widely used geometry for the micro-strip patch antenna. As in rectangular

micro-strip antenna we have two degree of freedom (length and width) to control the antenna characteristics, here we have only radius of circular patch [22].

2.2 Antenna geometry

The geometry of the co-planar investigated antenna [20] is shown in figure 2.1. Assumed to be a 0.035 mm thin copper metallic and the circular radiating patch has a radius of 15mm. The FR4 substrate material thickness is 1.6 mm with a relative permittivity of 4.3 and a loss tangent of 0.0017. The antenna external dimensions are 50 mm width and 50 mm length.

The excitation is achieved using a 50-ohms transmission line with strip thickness of 3 mm, a length of 13.6 mm and a gap distance of 0.5 mm between the strip and the co-planar ground plane. The ground plane is a rectangular strip with a width of 23mm and a length of 13 mm.

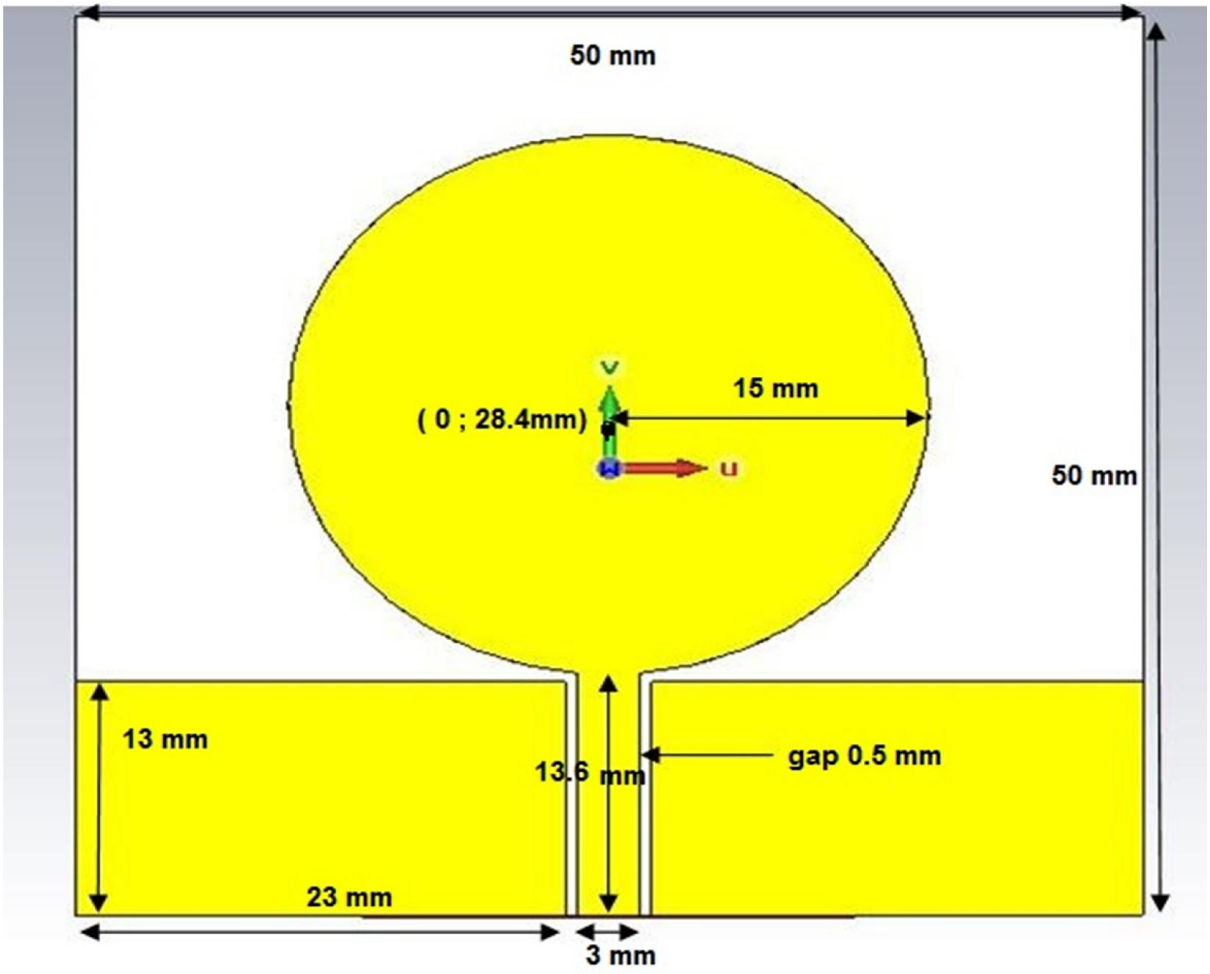

Figure 2.1.a 2-D view of the co-planar investigated PCMA.

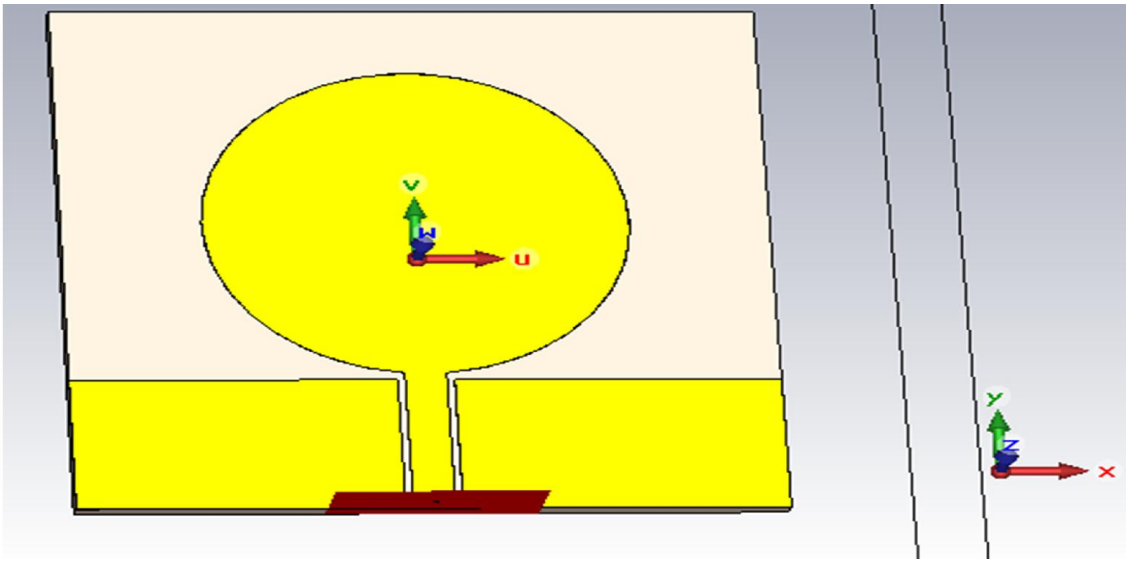

Figure 2.1.b 3-D view of the investigated PCMA.

2.3 simulated results

- **Return loss**

The return loss versus frequency for the original structure parameters is shown in figure 2.2 below:

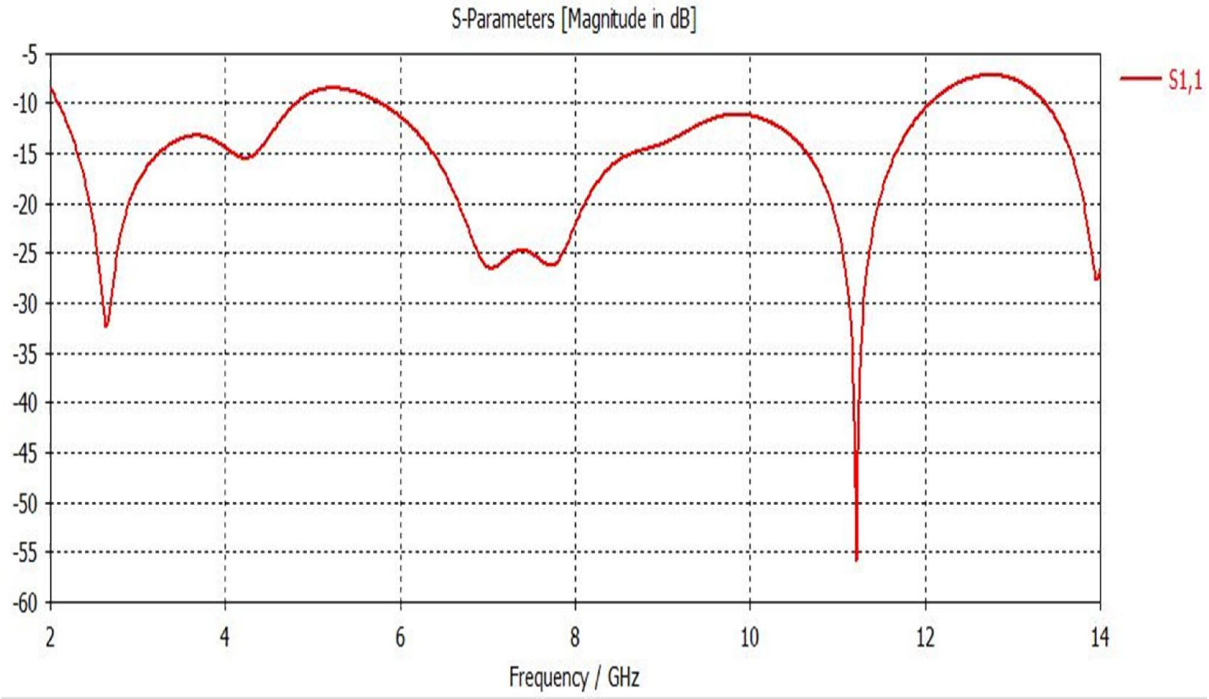

Figure 2.2 return loss versus frequency.

We notice two sharp resonance frequencies 11.22 GHz and 2.6467 GHz. Also, over the frequency range extending up to 14 GHz, the structure exhibits a multiband behavior since the return loss level is lower than -10 dB over the frequency bands [2.09 GHz – 4.806 GHz], [5.768 GHz – 12.051 GHz] and [13.369 GHz– over than 14 GHz].

- **Voltage Standing Wave Ratio**

Figure 2.3 shows the VSWR of the antenna.

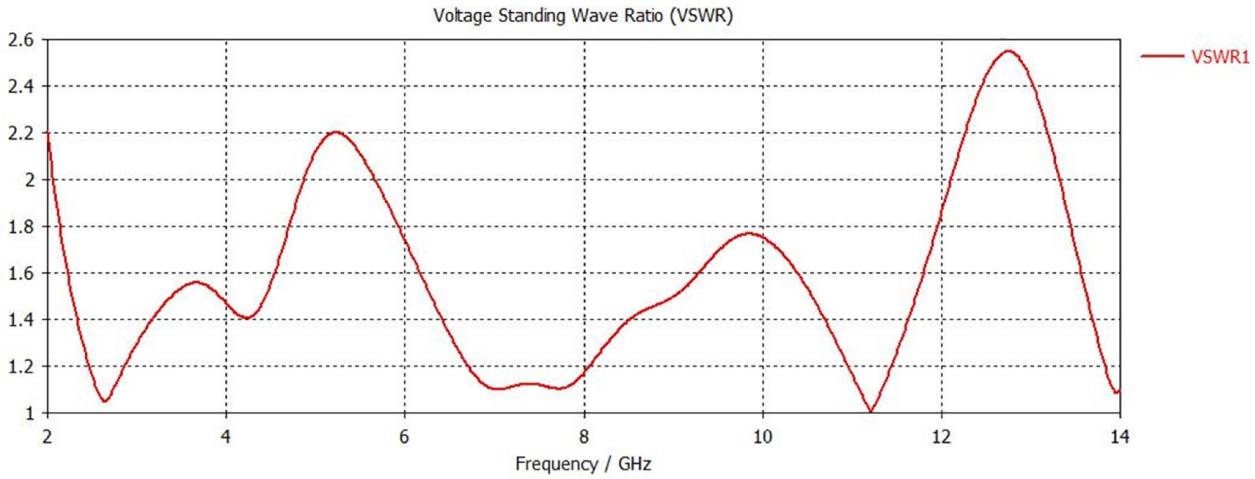

Figure 2.3 VSWR of the PCMA proposed antenna.

The antenna VSWR graph shows that the minimum values are at the peak and maximum values are at the resonant frequencies (2.6467 GHz and 11.22 GHz).

- **Input Impedance Z_{11}**

The antenna input impedance real and imaginary parts are shown in Figures 2.4 and 2.5 respectively. We note that at the resonant frequencies the imaginary part is null and the real part is around 50 Ohms achieving a good power matching at the considered feeding point.

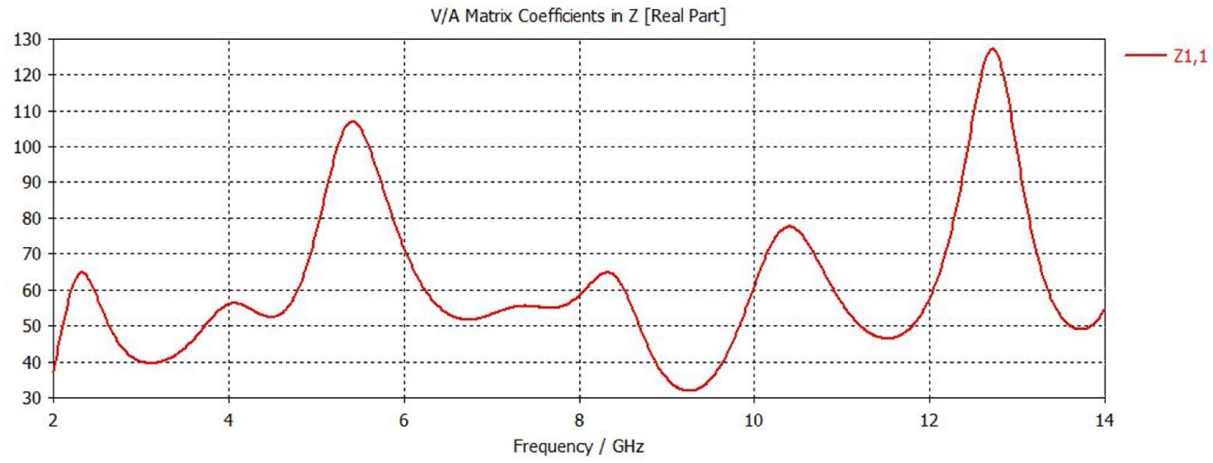

Figure 2.4 Real part of Z_{11}

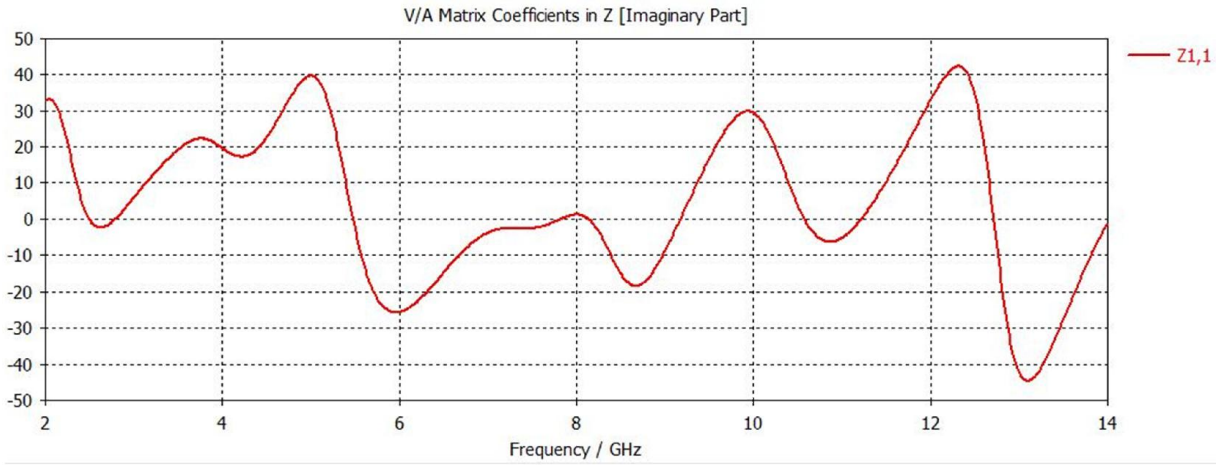

Figure 2.5 the imaginary part of Z_{11}.

- **Current distribution**

The normalized current density distribution of the considered antenna at the resonant frequencies 2.6467 GHz and 11.22GHz are illustrated in Figure 2.6 and Figure 2.7.

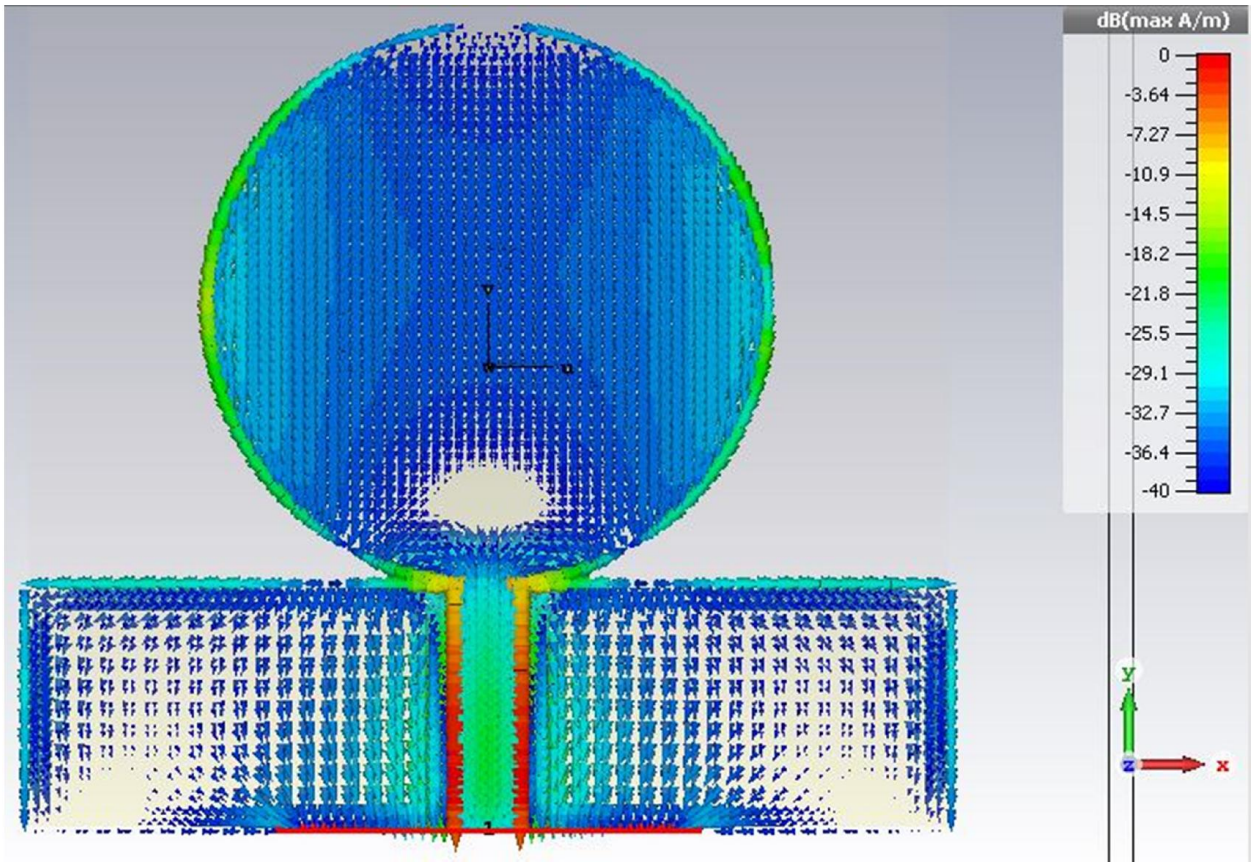

Figure 2.6 Current distribution of the resonant frequency 2.6467 GHz.

As can be observed from this figure, the current density is concentrated along the whole circular patch but more strong values at the left and the right sides and it is weak at the lower and top sides of the patch.

Moreover, the current density is much stronger at the edges of the circular patch and start decreasing at the upper edges.

The current density is maximum at the gaps between the ground and the micro-strip line with 0 dB. As can be seen, there is current distribution symmetry along the direction of the current because of the symmetry of the patch.

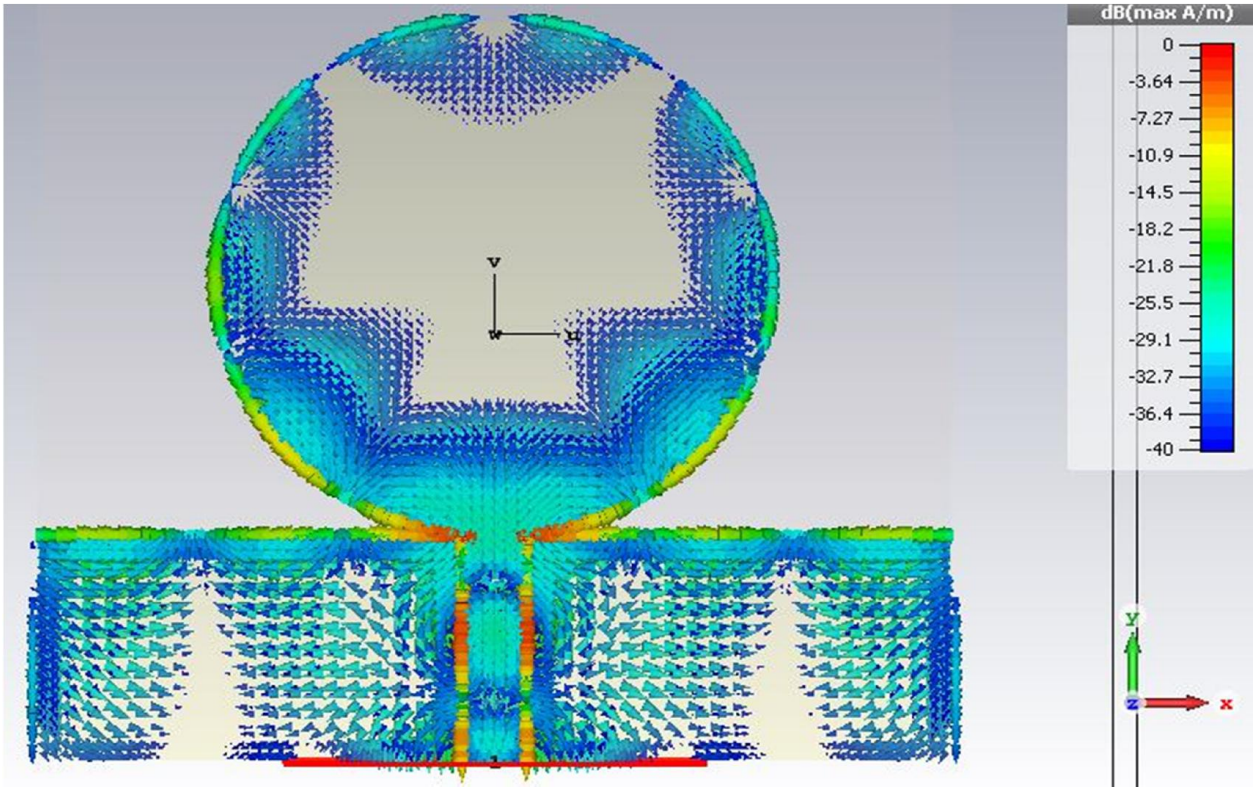

Figure 2.7 Current distribution of the resonant frequency 11.22 GHz.

As can be observed from this figure, the current density is concentrated around the edges of the circular patch and start decreasing gradually as we move to the center of the patch and almost absent at the center of the patch.

Moreover, the current density is maximum at the lower edges of the circular patch and start decreasing at the upper edges with some turbulence of values and directions in the range of -2 dB to -30 dB.

As we see, there is a current distribution symmetry along the direction of the current because of the symmetry of the geometry shape.

- **2-D Far Field Radiation Pattern**

The simulated far field radiation patterns of the original antenna at the sharp resonant frequencies are shown below.

The radiation pattern information (main lobe magnitude, direction and beam width) at both frequencies and in both E and H planes are indicated near to the graph.

- E-plane (φ= 90°plane)

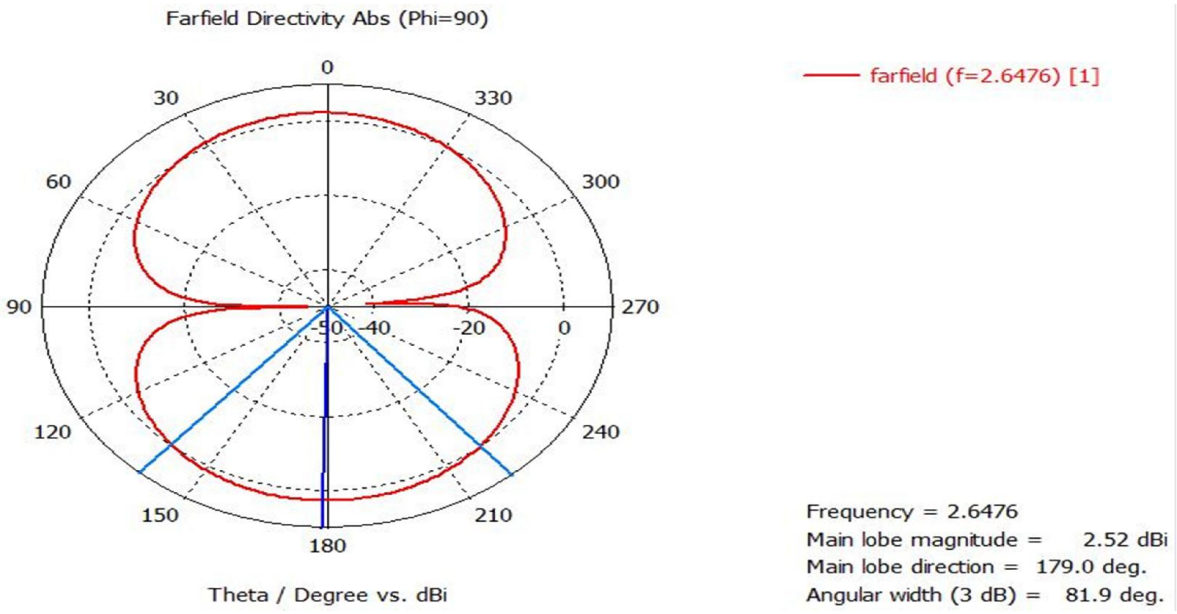

Figure 2-8-a E-plane radiation pattern at 2.6476GHz.

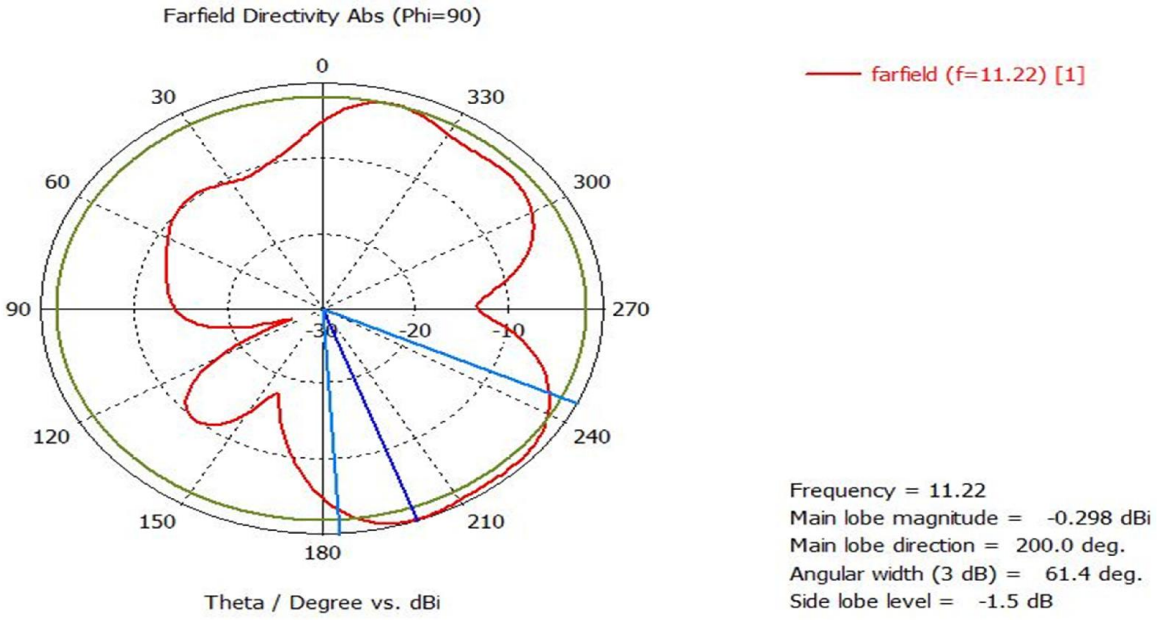

Figure 2-8-b E-plane radiation pattern at 11.22 GHz.

- **H-plane (φ= 0°plane)**

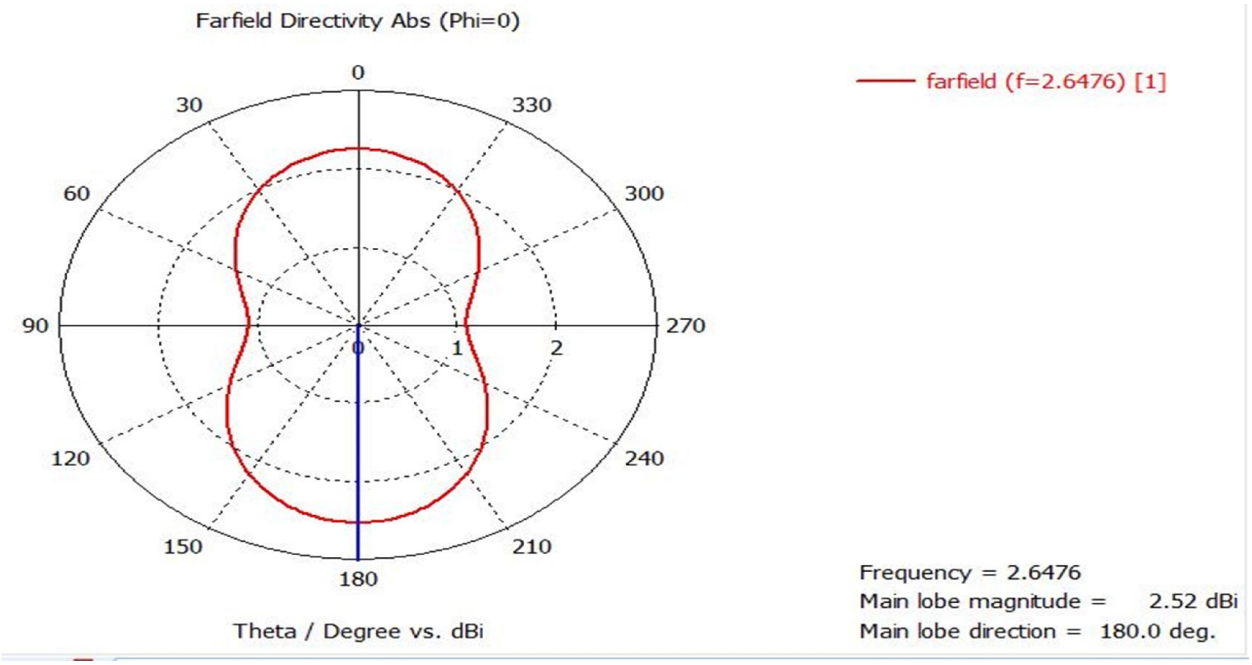

Figure 2-9-a H-plane radiation pattern at 2.6476 GHz.

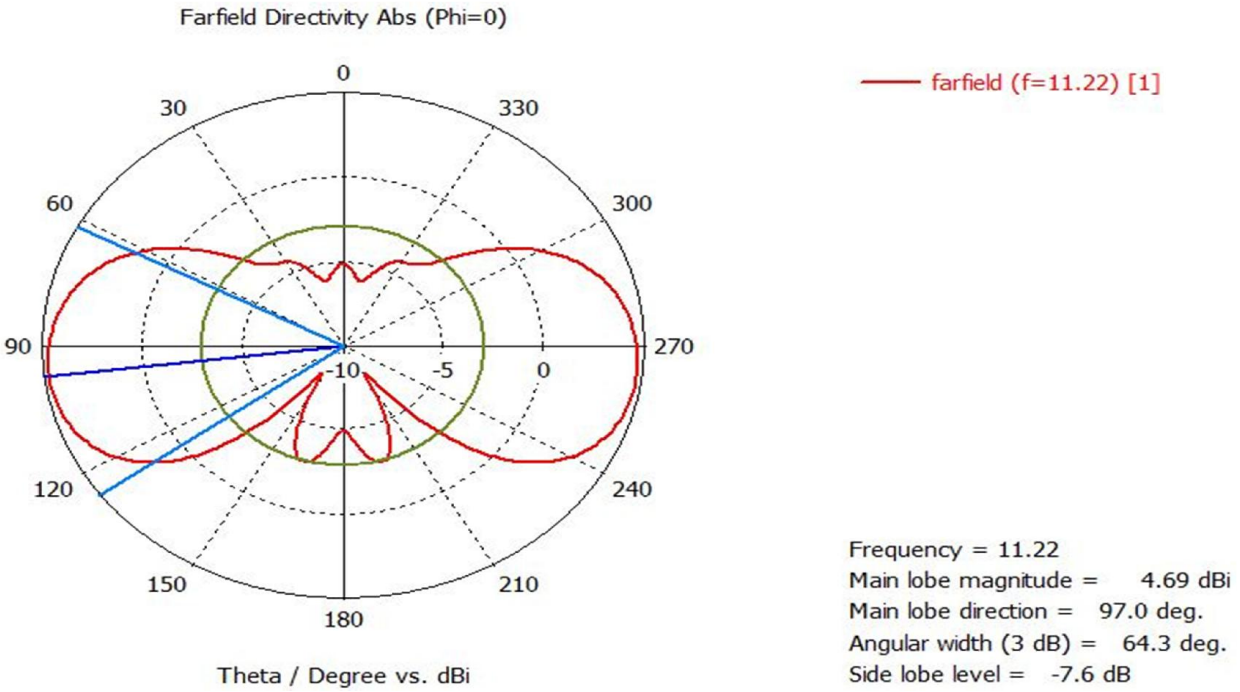

Figure 2-9-b H-plane radiation pattern at 11.22 GHz.

- **The 3-D radiation pattern**

The 3D radiation patterns of the structure and both frequencies are shown below. It is seen in this figure that the monopole antenna radiates in both sides of the planar patch as opposed to a conventional microstrip antenna.

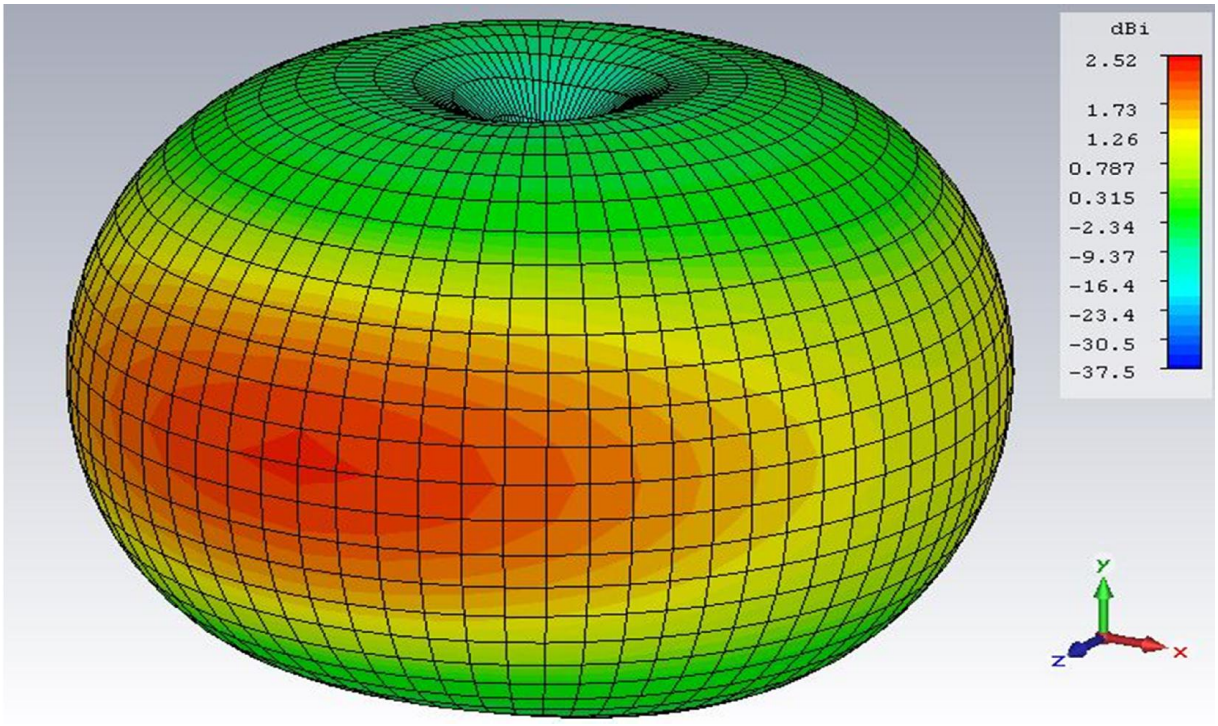

Figure 2.10.a The 3-D radiation pattern (f=2.6476 GHz).

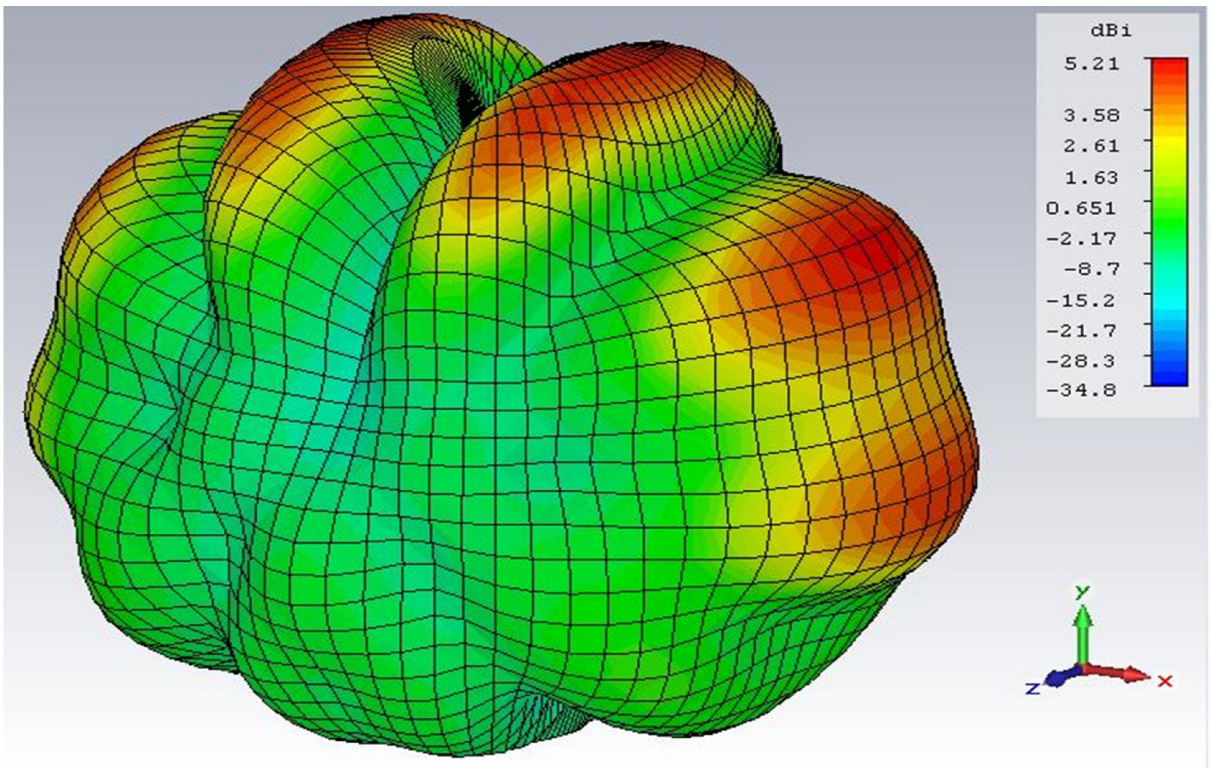

Figure 2.10.b The 3-D radiation pattern (f=11.22 GHz).

2.4 Conclusion

The analysis achieved in this chapter verifies that the considered structure in [20] is a tri-band antenna. Moreover, analysis of its radio electric properties is performed at two peak resonant frequencies. In the next chapter, modification will be introduced to develop an ultra-wide band printed monopole antenna.

Chapter three

Ultra Large Band Printed Monopole Antenna

In this chapter, a defected antenna obtained from the previous investigated structure has been obtained. This is mainly achieved by inserting defects in specific locations of the patch which resulted in vanishment of tri-band properties. Furthermore, the obtained final defected structure shows the desired ULB characteristic.

3.1 Effect of defects on PCMA

3.1.1 Antenna description

Figure 3.1 illustrates the new shape that has been extensively modified at two levels. In first step, physical parameters related to available material in the telecommunication laboratory were introduced (h= 1.63 mm; εr = 4.3 and loss tan = 0.0017).

In second step, circular shaped defects were introduced as shown in 3.3. Some shape defects on the top to push down the current flow and in the right and the left edges maximum current density of the patch according to the investigated structure current density. Alike the antenna geometry investigated in chapter 2, this antenna is symmetrical with respect to y axes achieving polarization along the plane φ=90°. The antenna parameters and shape are shown in figures 3.2 and 3.1 respectively. The defects characteristics are detailed in the next section.

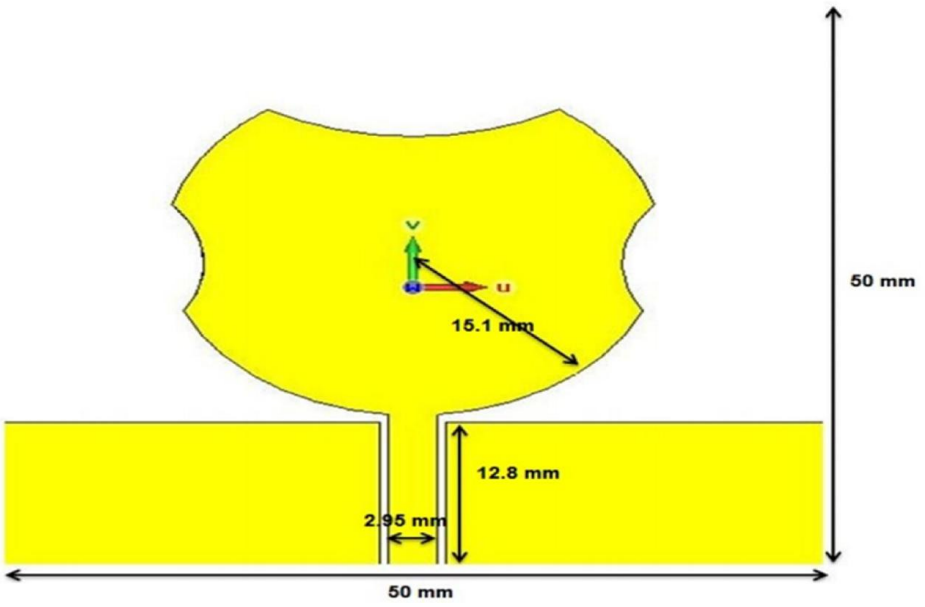

Figure3.1 2-d front view of the new shape.

Parameter List

Name	Expression	Value	Description	Type
a	= 50	50	substrate length	Length
b	= 50	50	substrate width	Length
m	= 13.6	13.6	microstrip length	Length
h	= 1.63	1.63	substrate height	Length
e	= 23	23	ground length	Length
l	= 12.8	12.8	ground width	Length
t	= 0.035	0.035	cooper thikness	Length
f	= 2.95	2.95	waveguide width	Length

Figure 3.2 New parameter values.

3.1.1.a Used circular defects

We realized our circular shaped defects on the antenna as shown in figure 3.3.

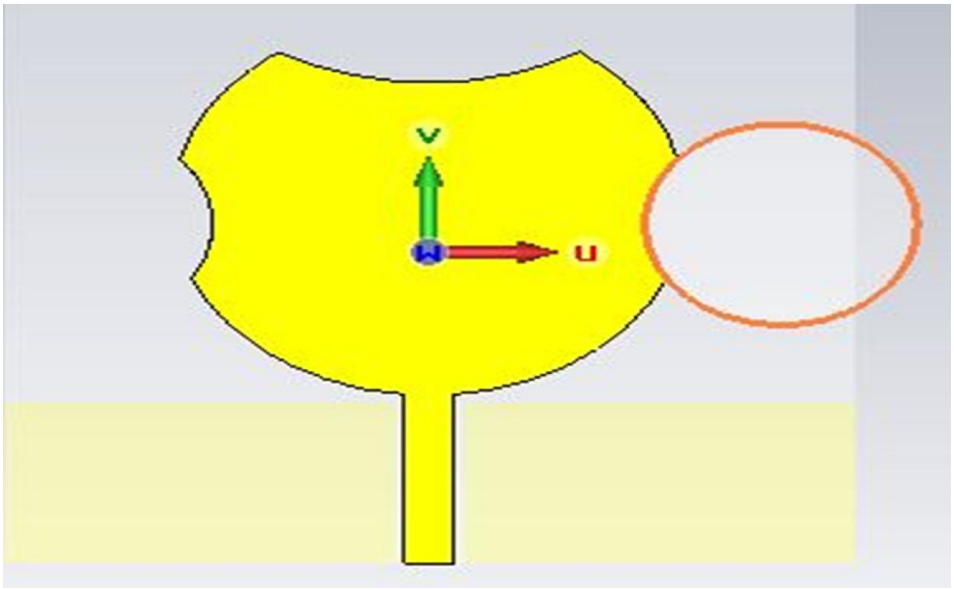

Figure3.3 2-d view defect realization.

Table 3.1positions of the complete defect cylinders.

	Radius	Center coordinates	
		u	v
Top cylinder	17.5 mm	0 mm	30.8 mm
Right cylinder	8 mm	20.7 mm	2 mm
Left cylinder	8 mm	-20.7 mm	2 mm

We used the 50 Ω microstrip line to match the radiating patch, after we tested many configurations, the one achieving maximum ultra large band frequency range and the lowest overall return loss below -10 dB is selected.

3.1.1.b Realized antenna

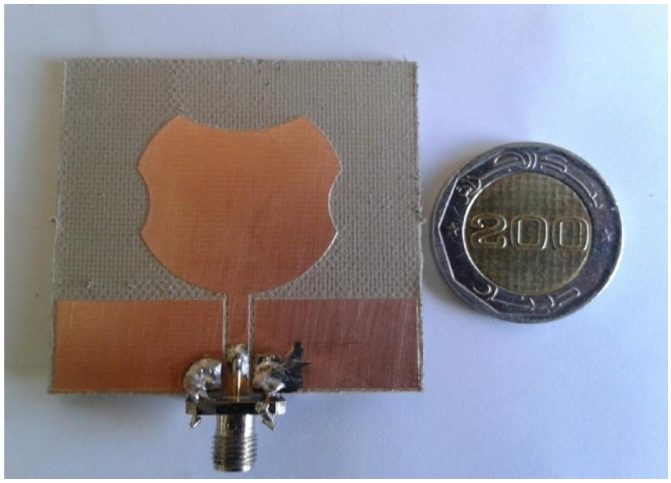

Figure 3.5 back Photograph of the antenna.

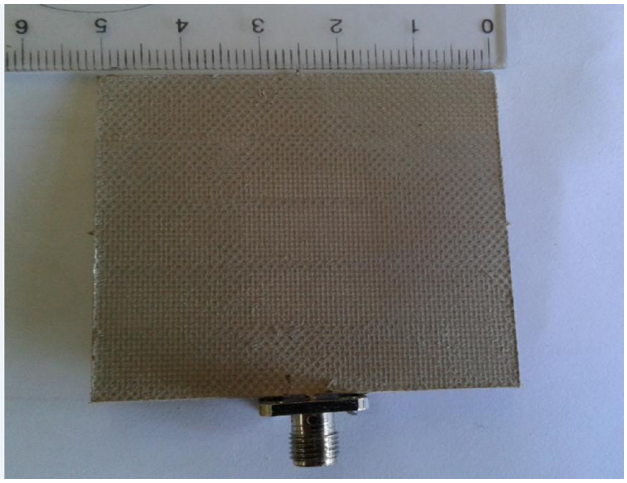

Figure 3.4 front Photograph of the constructed antenna.

3.2 Simulated results

- **Return loss**

After inserting the defects into the investigated PCMA, we noticed the drop of the return loss graph at the frequency ranges from 4.806 GHz to 5.768 GHz and from 12.051 GHz to 13.369 GHz below the -10 dB level in the simulated result. Also it has been found that minimum return loss is RL= -31 dB which means a good impedance matching at that frequency.

After constructing the new antenna in the institute telecommunication laboratory we performed our measurement using ROHDE and SCHWARDZ ZNB 20 vector network analyzer operating in [100 kHz -20 GHz] frequency range. The measured and the simulated results are shown in figure 3.6.

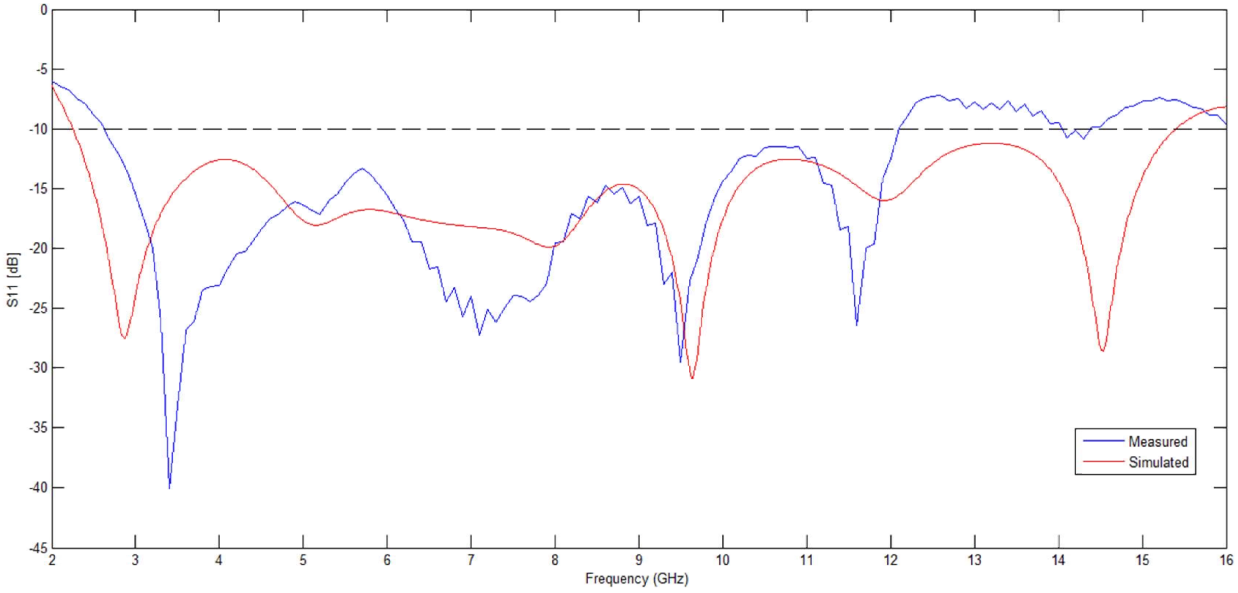

Figure 3.6 measured and simulated return losses versus frequency.

Table 3.2 comparison of simulated and measured results.

	Frequency high (GHz)	Frequency low (GHz)	Frequency center (GHz)	%BW
Simulated	15.4	2.253	8.83	149%
Measured	12.15	2.6	7.375	129%

We notice a small positive shift of the measured results compared to the simulated ones at the lower band limit and a negative shift at the high band limit. Also, both simulated and measured bands show that the developed monopole antenna is an Ultra Large Band structure. This figures shows that the antenna structure presents peak resonant frequencies with minimum reflection coefficients. Finally, we note a quite similar shape of the return loss over the entire bandwidth.

- **Voltage Standing Wave Ratio (VSWR)**

Figure 3.7 shows the VSWR takes the maximum values nearly 1 at the resonant frequencies

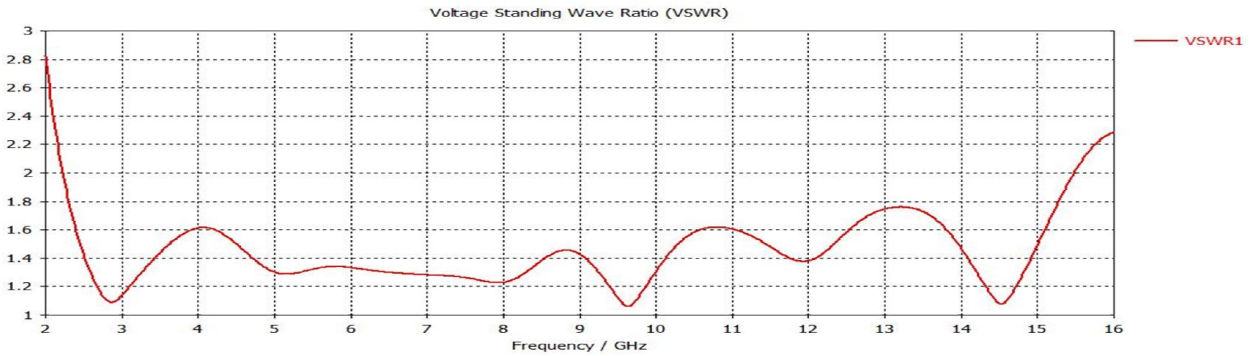

Figure 3.7 voltage standing wave ratio versus frequency.

The antenna VSWR graph in figure 3.7 shows that the minimum values are at the peak of the graph and maximum values near to 1 are at the resonant frequencies (2.8692 GHz, 9.6283 GHz and 14.531 GHz).

- **Input impedance**

figure 3.8.a and 3.8.b show the input impedance satisfies good matching condition at the resonant frequencies since the real part is close to 50Ω, whereas the imaginary part is close to zero.

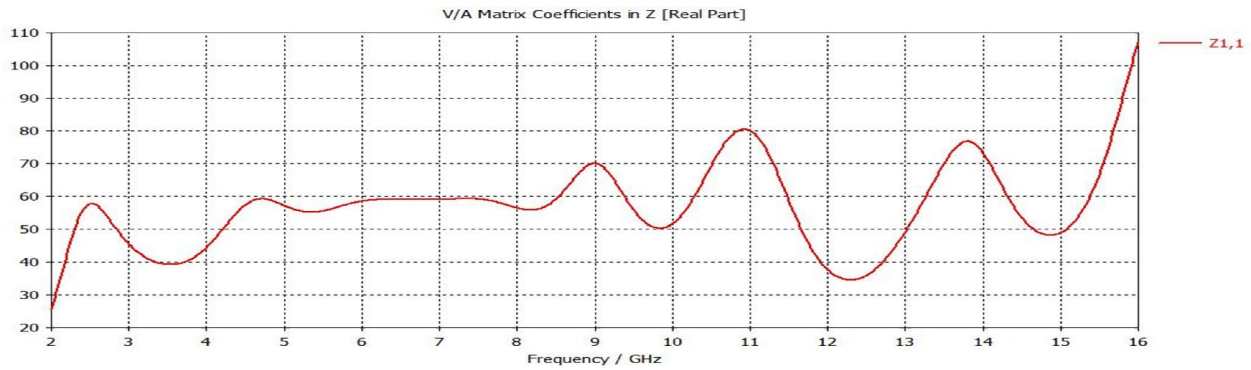

Figure 3.8.a real impedance versus frequency.

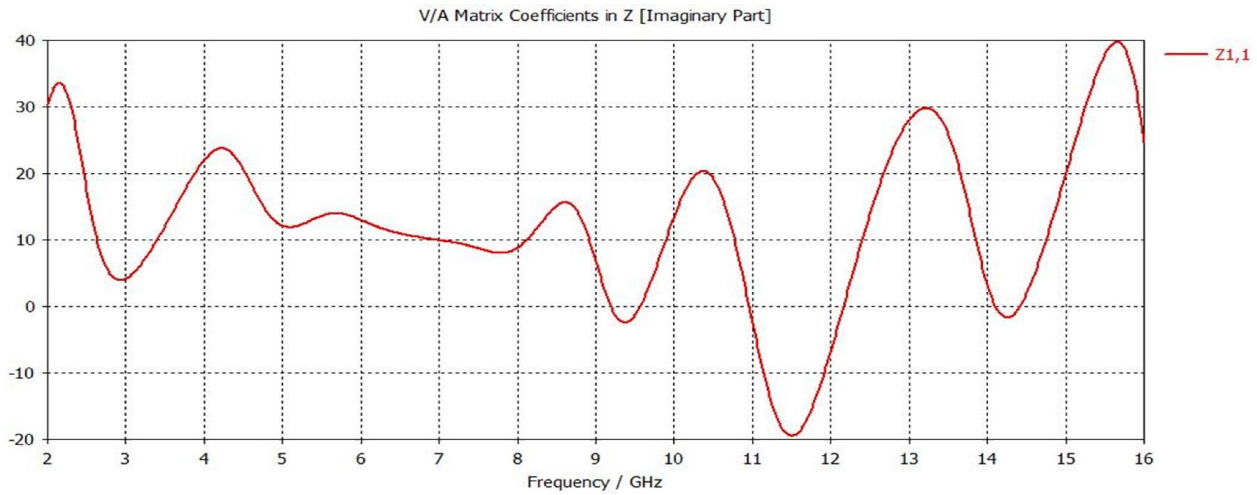

Figure 3.8.b imaginary impedance versus frequency.

- **Current distribution**

Figure 3.9 (a-b-c) show the modified PCMA current density distributions at the three peak resonances. The performed modification has an effective impact on the current distribution on the antenna propriety.

We notice a symmetrical current density distribution on the patch. The density is higher at the antenna left and right edges near the defect and in the lower side whereas it is minimum elsewhere. Therefore, we explain the increase of the bandwidth of the frequency by the current path modification due to the defects which force the current to take a different path.

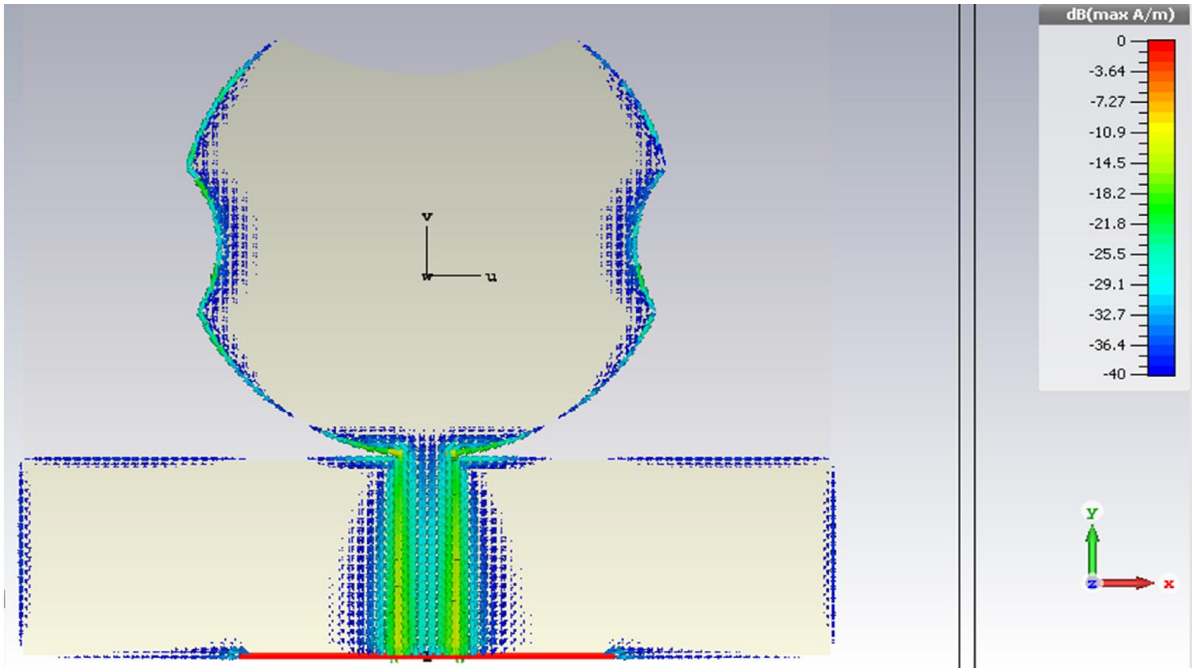

Figure 3.9.a current distribution at f = 2.8692 GHz.

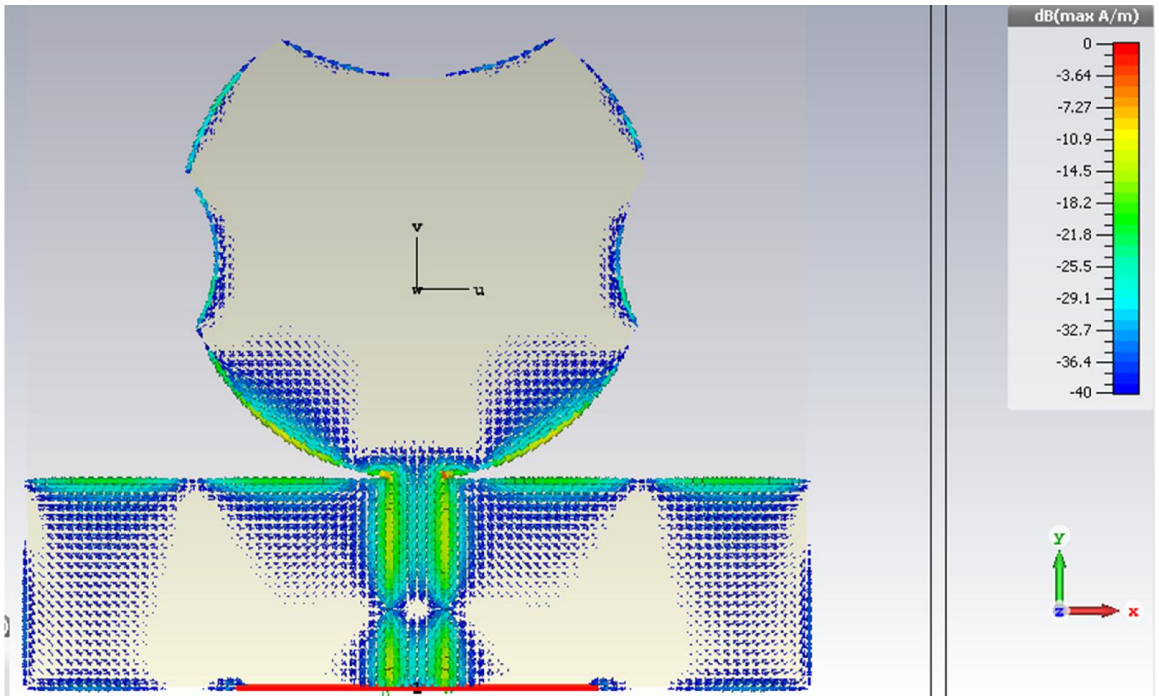

Figure 3.9.b current distribution at f = 9.6283 GHz.

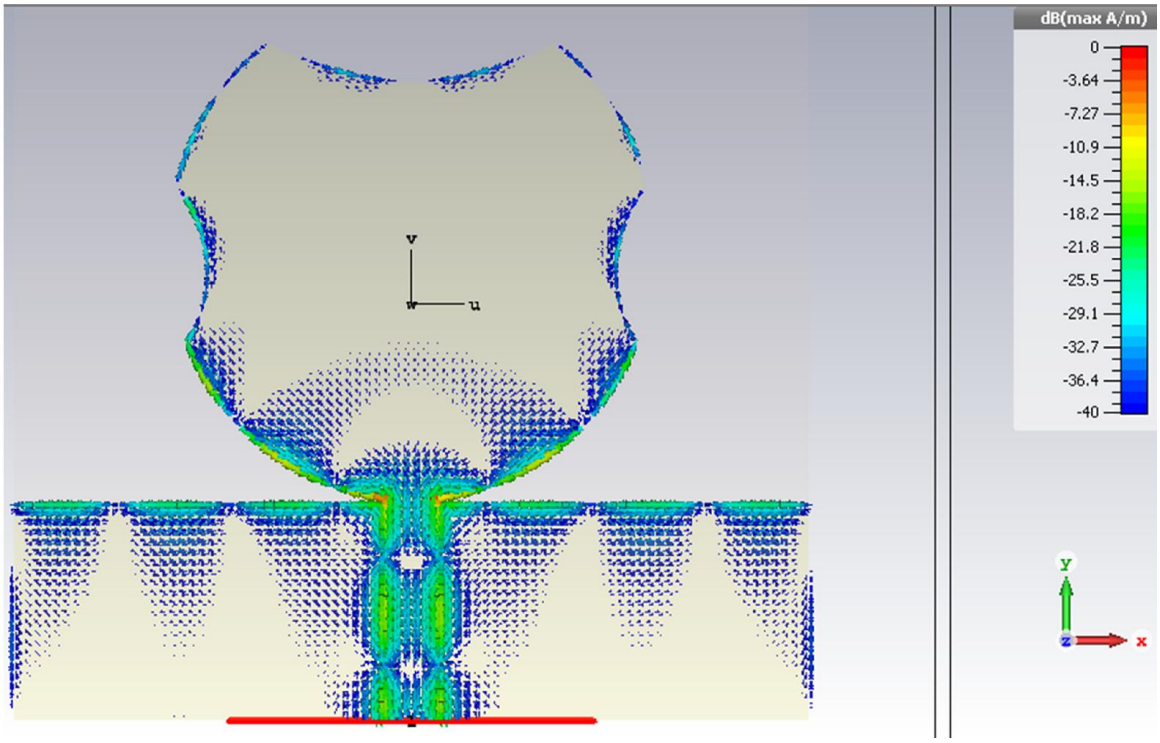

Figure 3.9.c current distribution at f = 14.531 GHz.

- **Radiation pattern**

The simulated far zone radiation patterns of the modified antenna at resonant frequency f=2.8692 GHz in the E-planes (φ= 90°) plane and H-plane (φ= 0°) are illustrated in Figure 3.10.a

and 3.10.b. The radiation pattern information (main lobe magnitude, direction and beamwidth) at both frequencies and in both E and H planes are indicated near to the graphs.

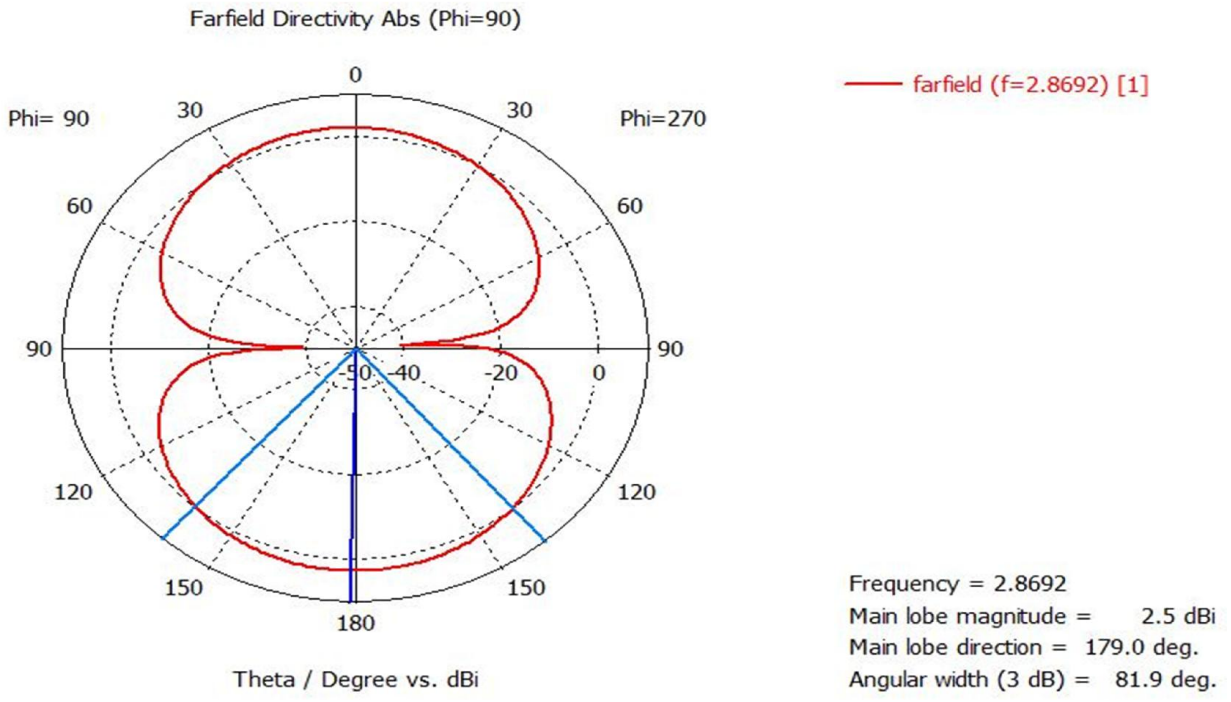

Figure 3.10.a simulated E radiation pattern at f = 2.8692 GHz.

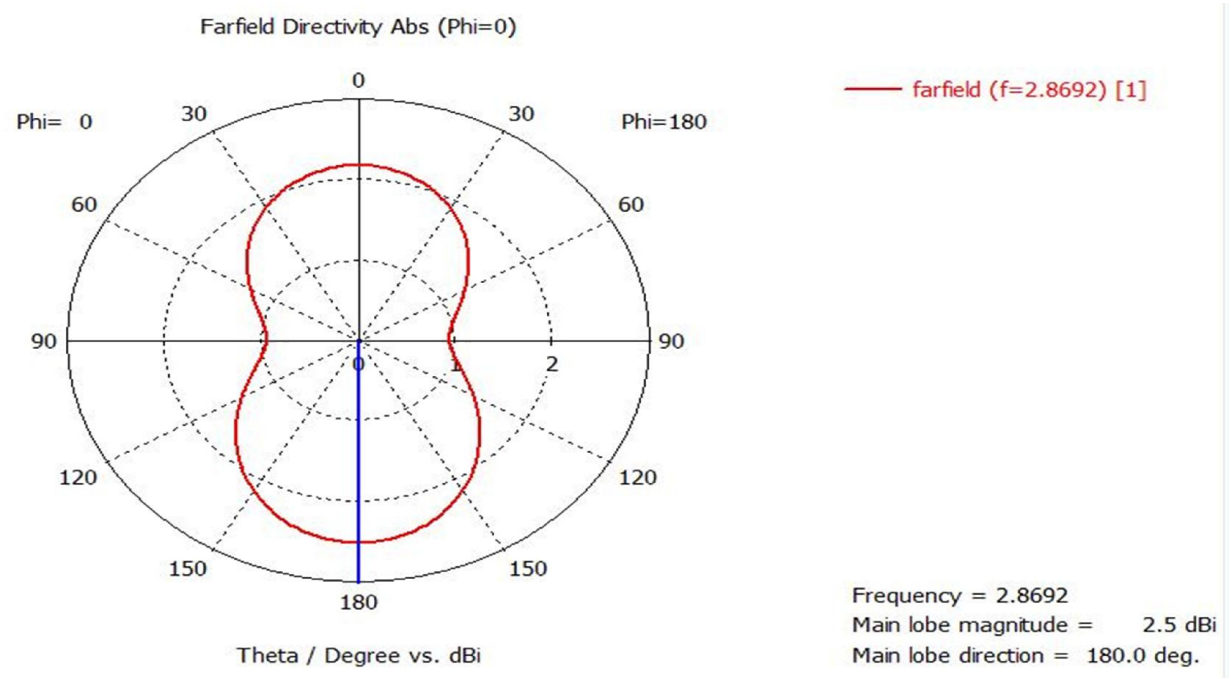

Figure 3.10.b simulated H radiation pattern at f = 2.8692 GHz.

The simulated far zone radiation patterns of the modified antenna at resonant frequency f=9.6283 GHz in the E-planes φ= 90° plane and H-plane (φ= 0°) are illustrated in Figure 3.11.a and 3.11.b.

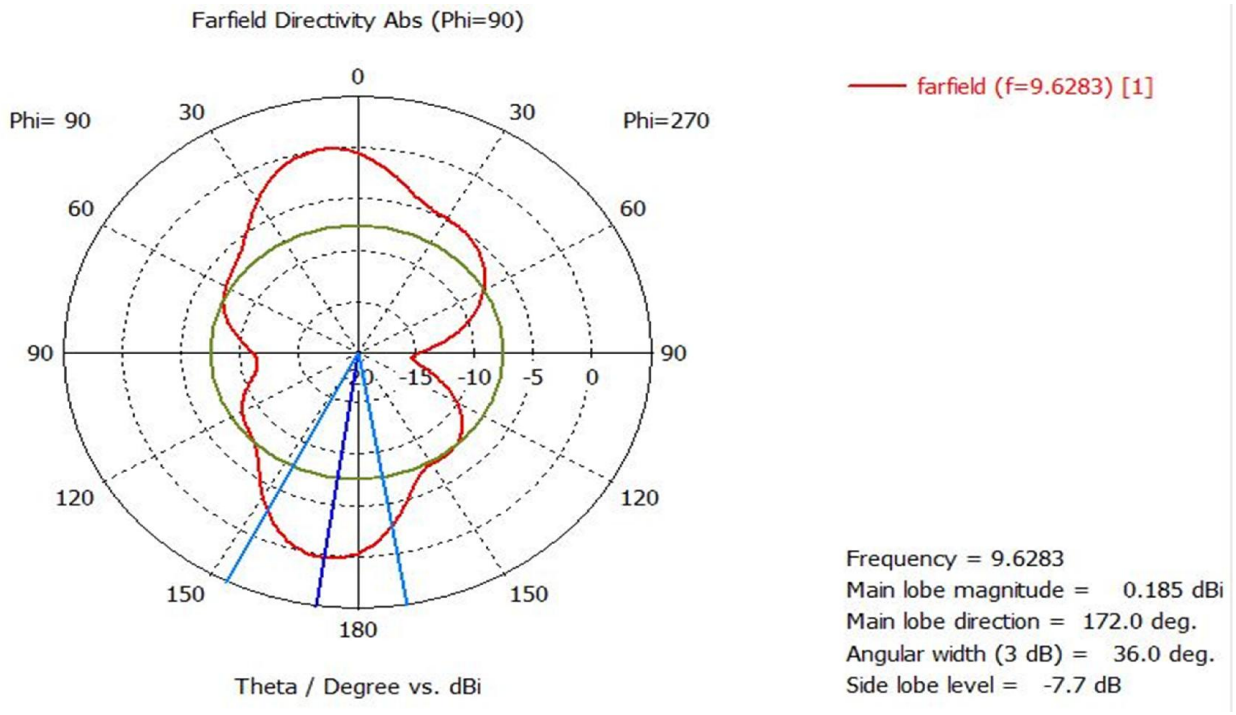

Figure 3.11.a simulated E radiation pattern at f = 9.6283 GHz.

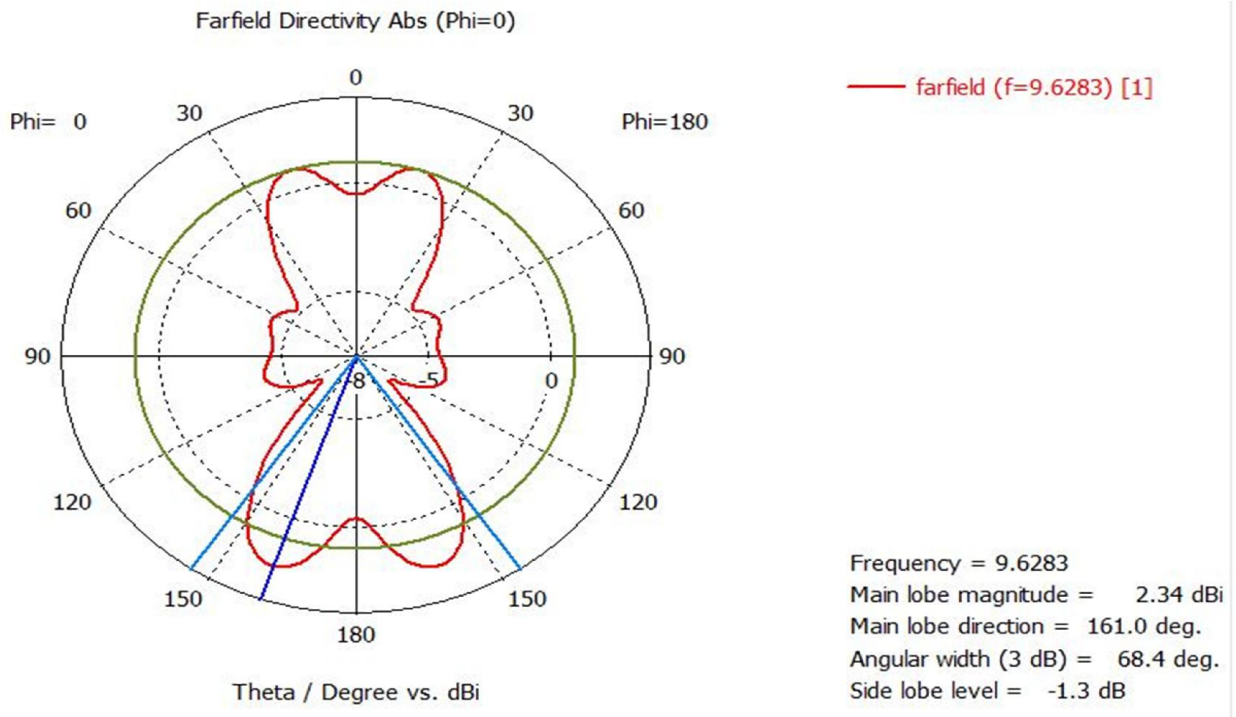

Figure 3.11.b simulated H radiation pattern at f = 9.6283 GHz.

The simulated far zone radiation patterns of the modified antenna at resonant frequency f=14.531 GHz in the E-plane (φ= 90°) and H-plane (φ= 0°) are illustrated in Figure 3.12.a and 3.12.b.

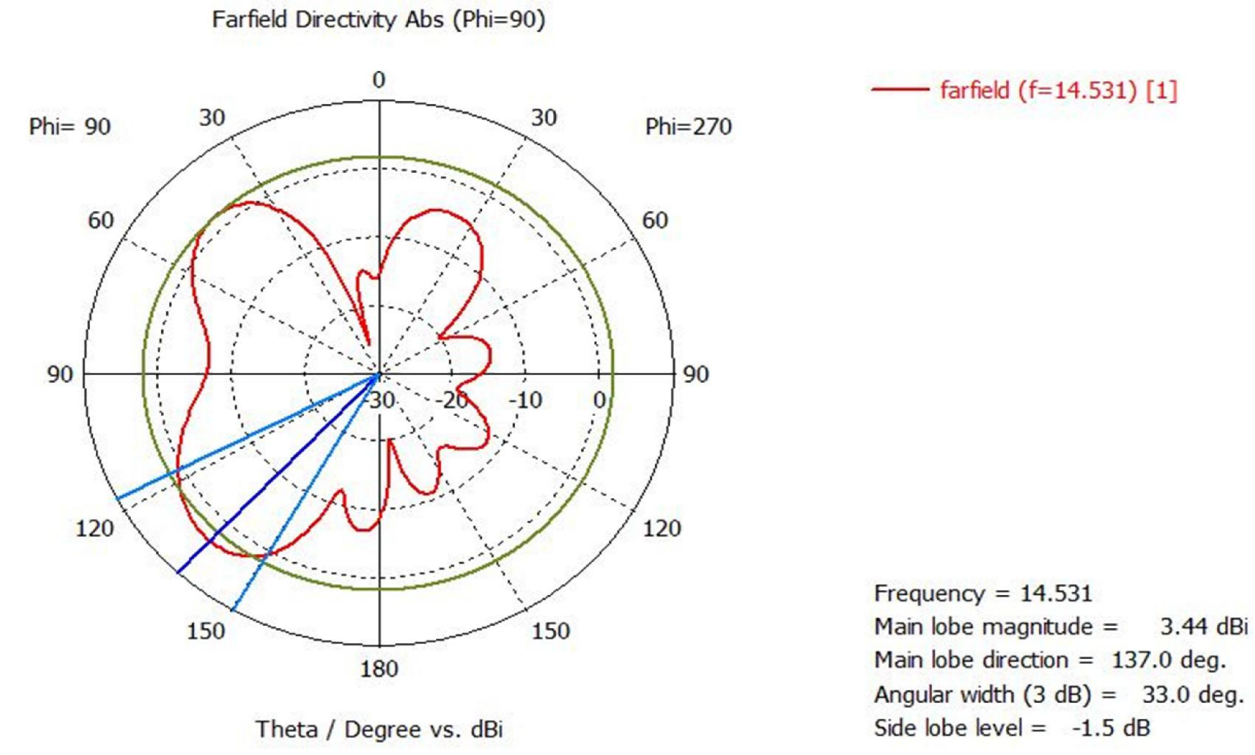

Figure 3.12.a simulated E radiation pattern at f = 14.531 GHz.

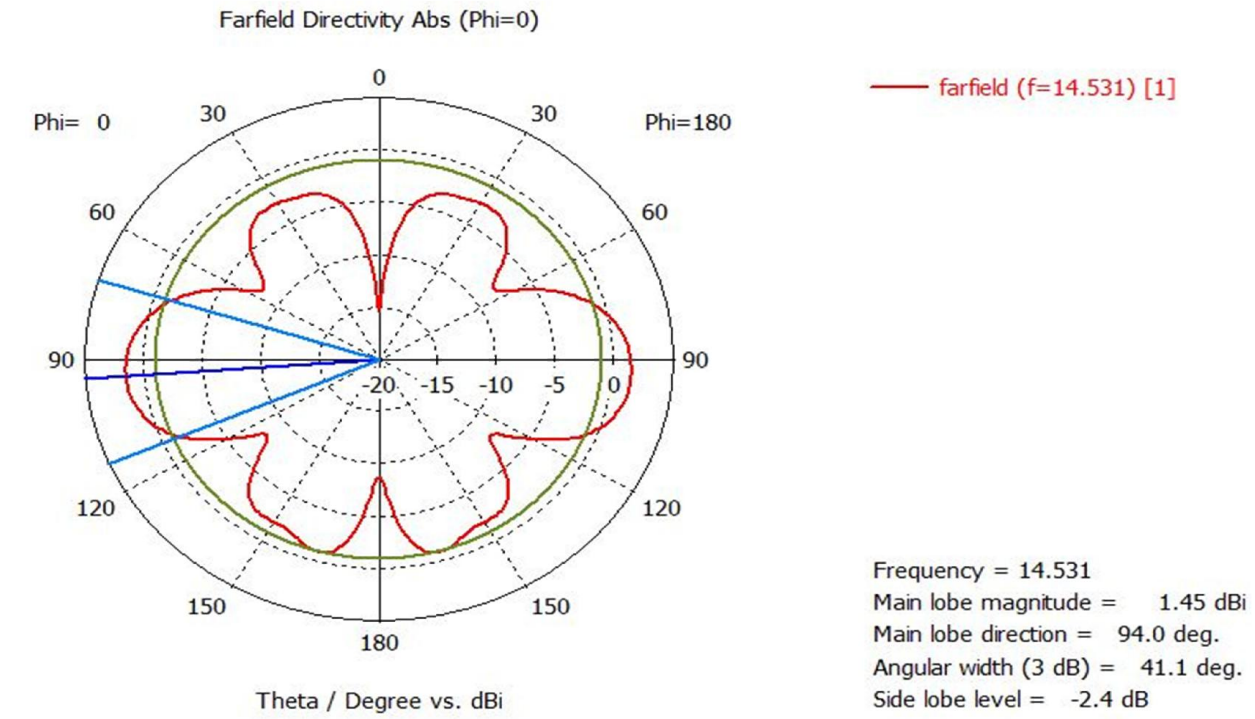

Figure 3.12.b simulated H radiation pattern at f = 14.531 GHz.

- From Figure 3.10, we note that the radiation patterns show two lobes in both *E* and *H*-planes with large beamwidths.

- From Figures 3.11 and 3.12, we note that the radiation patterns show side lobes in both *E* and *H*-planes with unsymmetrical radiation pattern.
- The 2-D patterns show that the antenna radiates in both side of the structure as expected from a monopole structure.

- **The 3-D radiation pattern**

The antenna 3-D radiation pattern plot is shown in Figure 3.13 (a,b,c)**.**

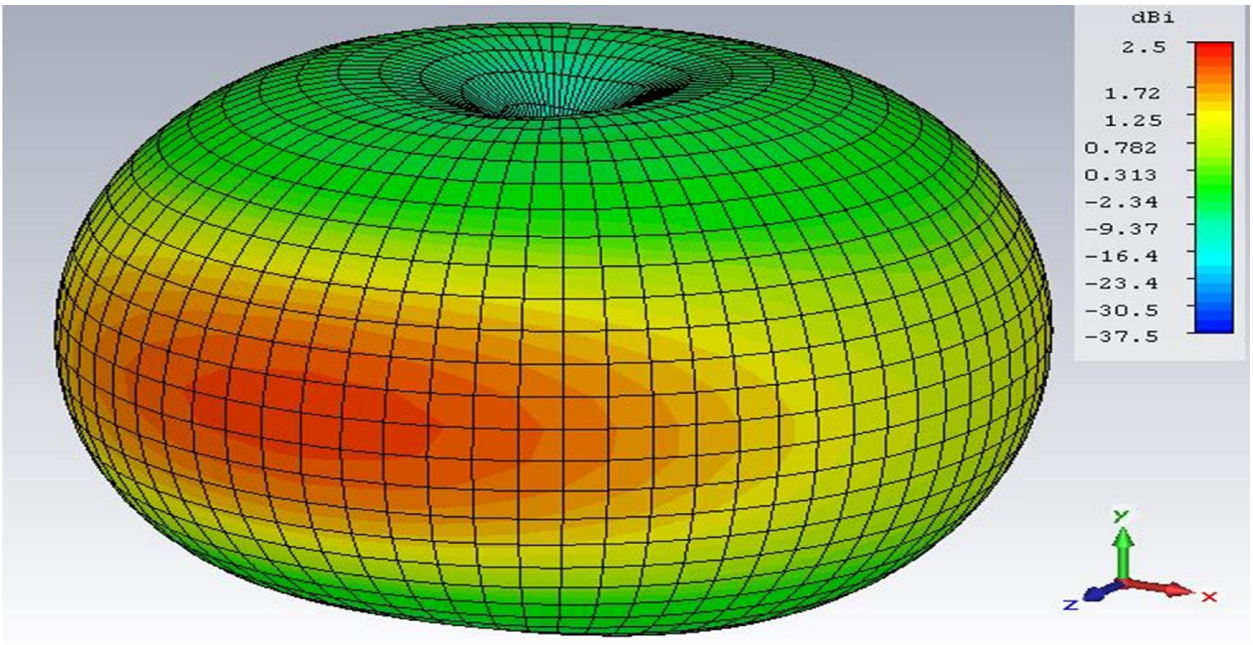

Figure 3.13.a 3-D radiation pattern at f= 2.8692 GHz.

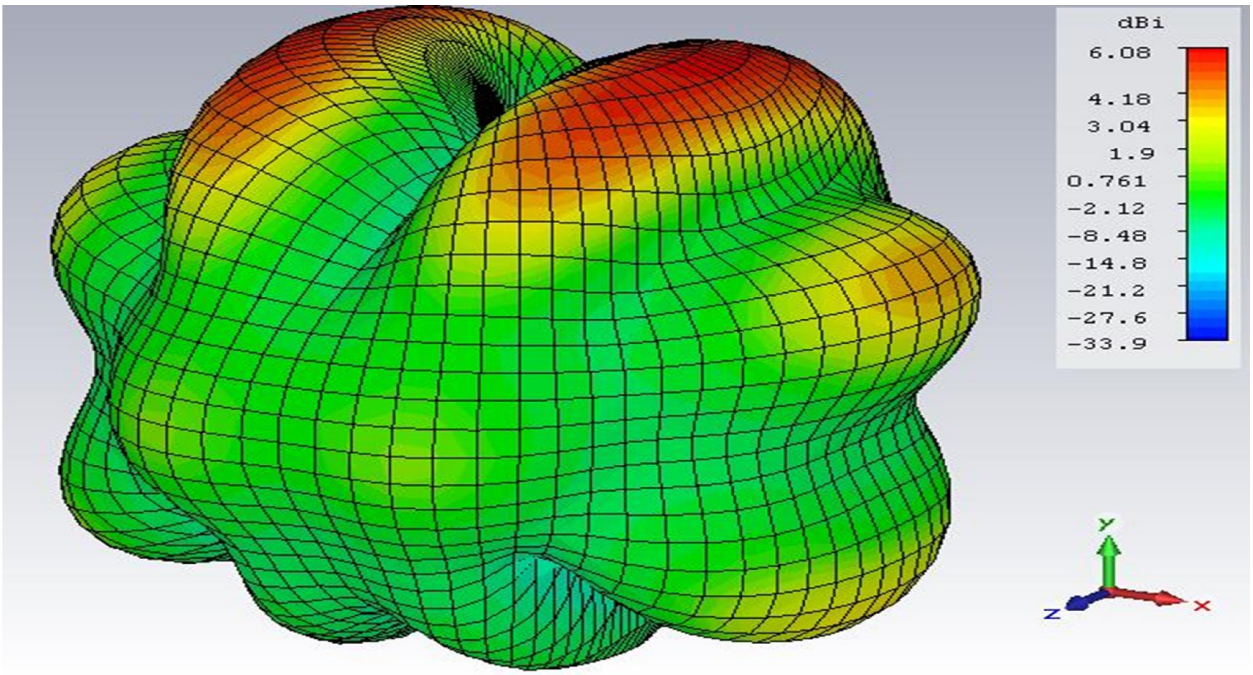

Figure 3.13.b 3-D radiation pattern at f= 9.6283 GHz.

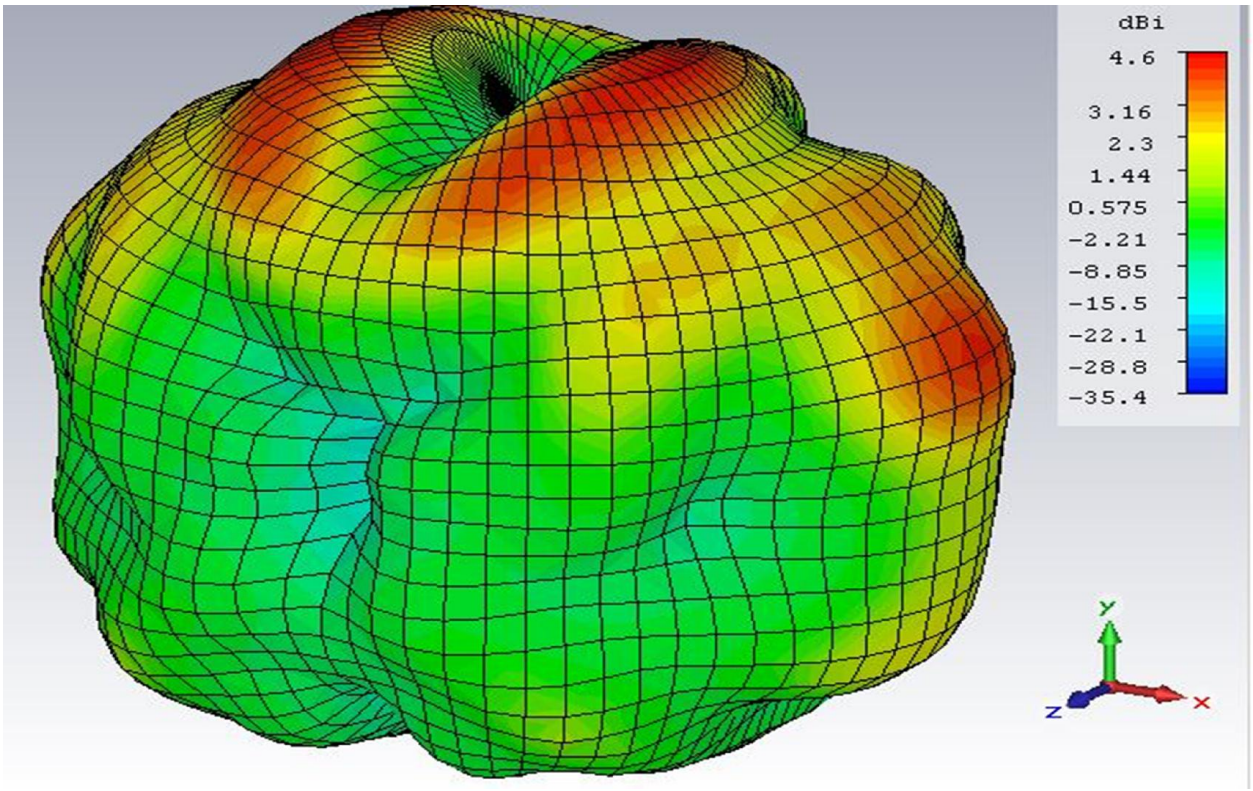

Figure 3.13.c 3-D radiation pattern at f= 14.531 GHz.

Table 3.3 directivity of the resonant frequencies

Resonant frequency (GHz)	Directivity (dBi)
2.8692	2.5
9.6283	6.08
14.531	4.6

.

3.3 Conclusion

In this chapter, a defected circular ULB monopole antenna has been developed on the basis of the PCMA structure investigated in the previous chapter. The obtained antenna has been fabricated and its reflection coefficient measured. A good agreement is observed with the simulated results. The measured antenna percent bandwidth is 129 % whereas the simulated one is 149%. The return loss results present a quite similar form over the frequency range where a good impedance matching was obtained.

The antenna can operate in the frequency range extending from 2.6 GHz to 12.15 GHz covering different frequency bands and suitable for various applications.

General Conclusion

The main objective of this work is to develop an Ultra Large Band printed monopole antenna using defects.

This has been achieved throughout the following steps:

- A printed multiband circular monopole antenna (PCMA) has been considered and investigated using the Computer Simulation Technology (CST) software.
- The investigated antenna is modified by inserting circular shape defects on the upper, left and the right edges of the circular radiating patch. This has resulted in a return loss drop below the -10 dB level from 2.253 GHz to 15.400 GHz frequency range. The antenna dimensions have then been changed to achieve ULB operation.
- The obtained structure has been fabricated and its reflection coefficient measured using a vector network analyzer.

A good agreement is observed between simulated and experimental results. The measured antenna percent bandwidth is 129 % whereas the simulated one is 149%. In addition, the antenna simulated and measured refection coefficients present a quite similar form over the frequency range where a good impedance matching is observed.

The antenna can operate in different frequency bands (S, C and X) and hence, it is suitable for the various applications covered by these bands.

Moreover, different radio electric properties including input impedance, current distribution as well as 2D and 3D radiation patterns are simulated using the CST Microwave Studio tool.

As a further scope, we suggest to perform the following tasks:

- Parametric study on the proposed defects to optimize the antenna characteristics.
- Introducing structure modification to enhance the performance, especially the bandwidth.

References

[1] Dhunish Kumar Roll, “Design and Analysis of Microstrip Antennas for Ultra-Wide Band Applications”, *National Institute of Technology Rourkela*, May 2014.

[2] Analysis of a Rectangular Monopole Patch Antenna, International Journal of Recent Trends in Engineering, November 2009.

[3] K.P. Ray, Y. Ranga and P. Gabhale, “Printed square monopole antenna with semicircular base for ultra-wide bandwidth”, *Electronics Letters*, 2007.

[4] Wu. Q., R. Jin, J. Geng, and J. Lao, “Ultra-wideband rectangular disk monopole antenna with notched ground”, *Electronics Letters*,2007.

[5] Ultra-Wideband and Miniaturization of The microstrip Monopole Patch Antenna with Modified Ground Plane for Wireless Applications Progress in Electromagnetics Research Letters, Vol. 10, 171–184, 2009

[6] M. Joshua Singh, M. Mishra, and P. Sharma, “Design and Optimization of Microstrip Patch Antenna”, *Tirthankara Mahaveer University Moradabad*, September – October 2013.

[7]D. Kumar, “Design and Analysis of Microstrip Antennas for Ultra-Wide Band Applications”, *National Institute of Technology Rourkela Rourkela*, May 2014.

[8] Fawzy Ibrahim, “Antenna and Wave Propagation Chapter 7 Microstrip Antennas”, *Electronics and Communication Department Misr International University*.

[9]Dr A. Azrar.: course handout of “Antenna and Propagation” for M02 telecommunication option students, *Institute of electrical and electronic Engineering, university of Boumerdes*, Algeria.

[10] N. A. Zakaria, A. A. Sulaiman, and M. A. A. Latip, “Design of a Circular Microstrip Antenna”, *IEEE International RF and Microwave Proceedings*, December 2008.

[11] C. A. Balanis, “Antenna Theory, Analysis and Design”, Third edition, *John Wiley and Sons, New York*, 2005.

[12] Bhartia, Bahl, “Microstrip Antenna Design Handbook”,– *ISBN 0-89006- Garg*, 2000.

[13] Dr. Anil Chitade, “Design and Analysis of Microstrip Patch Antenna Using Meta material”, *INTERNATIONAL SOCIETY OF THESIS PUBLICATION*,2012.

[14] S. K. Behera, “Novel Tuned Rectangular Patch Antenna as a Load for Phase Power Combining”, PhD Thesis, *Jadavpur University*, Kolkata.

[15] G. Ramesh, “Microstrip antenna design handbook”, *Artech house*, 2001.

[16] P. Ramachandran, T.S. Keshav, L. M. Parupalli and S. Chakravarty, ‘‘On Antenna Design Simulation and Fabrication’’, PhD Thesis, *Deemed University*, Nagpur – India 2007.

[17] X.C. Yin, C.L. Ruan, C.Y. Ding, and J.H. Chu, ‘‘A Planar U Type Monopole Antenna for UWB Applications’’, *University of Electronic Science and Technology of China,2008*

[18] Ben Allen, M. Dohler, E. E. Okon, W. Q. Malik, A. K. Brown, and David J. Edwards, “Ultra-Wideband Antennas and Propagation for Communications, Radar and Imaging.

[19] M. K. A. RAHIM, T. MASRI, H. A. MAJID, O. AYOP, and F. ZUBIR, “Design and Analysis of Ultra Wide Band Planar Monopole Antenna’’, *Radio Communication Engineering Department Faculty of Electrical Engineering University Technology Malaysia.*

[20] MANSOURI Ali, “Reconfigurable Frequency Antenna Conception”, *Doctorate thesis telecommunication department, ecole national poly-technique*, Algeria ,2016

[21] Monopole antenna - Wikipedia, the free encyclopedia.

[22] D. J. Barasara, J. C. Prajapati, and A. M. Dethalia, “Multi frequency Fractal Antenna”, *International Journal of Scientific and Engineering Research*, Volume 3, Issue 7, July-2012.

[23] The evolution in 3D EM simulation software Version 2006 B – New Features.

[24] CST STUDIO SUITE 2015/Online Help/cst_studio_suite_help.htm.

Appendix

CST MICROWAVE STUDIO is a specialized tool for the fast and accurate 3D EM simulation of high frequency problems. Along with a broad application range, it offers considerable product-to-market advantages: shorter development cycles; virtual prototyping before physical trials; optimization instead of experimentation [23].

Since its inception in 1998, CST MWS has become renowned for its easy to use graphical interface and modeling abilities. It has remained the industry leading example of how to make3D EM simulation easy and efficient. Customers ranging from sole proprietors to large corporations have seen tremendous design cycle improvements and profited from an excellent return on investment [23].

With the successful introduction of the proprietary PERFECT BOUNDARY APPROXIMATION [PBA], CST created a significant technical advantage which has helped ensure its leadership in time domain simulation. Time Domain in combination with PBA has not only advantages in terms of speed but can also deliver accurate broadband time signals which are essential for TDR and signal integrity problems. But no one method is perfect for every application [23].

CST is the first commercial vendor to offer an HF 3D EM code which unites hexahedral and tetrahedral meshing, Time and Frequency Domain in one interface. Users can now switch easily from one to the other solver without changing the model and parametric settings and in this way benefit from the most appropriate method for each problem [23].

- **Time Domain Solver:**

A time domain solver calculates the development of fields through time at discrete locations and at discrete time samples. It calculates the transmission of energy between various ports or other excitation sources and/or open space of the investigated structure. Consequently, a time domain solver is remarkably efficient for most high frequency applications such as connectors, transmission lines, filters, antennas etc. and can obtain the entire broadband frequency behavior of the simulated device from a single calculation run.

In CST MICROWAVE STUDIO two-time domain solvers are available. One is based on the Finite Integration Technique (FIT), just called Transient solver, the second one is based on the Transmission Line Method (TLM) and is referred to as TLM solver. Both solvers work on hexahedral grids, however, the mesh setup is slightly different and classified as *Hexahedral* and *Hexahedral TLM* mesh type, respectively.

- Fast PBA mesher, with improved performance and robustness in particular for large imported models.
- New sub gridding scheme with improved flexibility of mesh subdivision, and drastically reduced memory requirements.
- Implementation of Linux version.
- Support of IEEE C 95.3 standard [SAR].[23]

- **Frequency Domain Solver:**

- Tetrahedral Frequency Domain solver with improved and more robust meshing algorithm.
- Excitation of fields by plane waves, multi-pin ports and waveguide ports on arbitrary planes in the model [slanted ports].
- Distributed computing scheme enables remote calculation.
- Upcoming Linux version.
- Easy access to surface currents, B and D fields.
- Improved mesh adaption for thin conductors.
- Solver performance increase for both direct [particularly out of core] and iterative solvers.
- Hexahedral and Tetrahedral Frequency Domain solvers 64 bit enabled

- **Adaptive mashing:**

The adaptive mesh refinement is an automatic scheme to create a mesh better suited for the given problem. With the refined mesh a new calculation ***pass*** will be started. Here, the initial mesh is automatically generated by the expert system and is used for the first pass calculation. Afterwards, the adaptive mesh refinement improves the mesh until the stop criteria are satisfied. As stop criteria, either the change in the S-parameters or the change of a user defined 0D result template from one pass to the next are available.

For the refinement of the meshes, two different strategies are available: The *energy based* mesh refinement stores the energy density distribution within the structure during a calculation. Based on these data, the mesh is refined afterwards in regions with high energy density. In contrast to this, the strategy based on the *expert system* successively changes the settings of the mesh expert system, so that finally an appropriate mesh is obtained that can be used afterwards for further parameter studies without activating the adaptive meshing again [24].

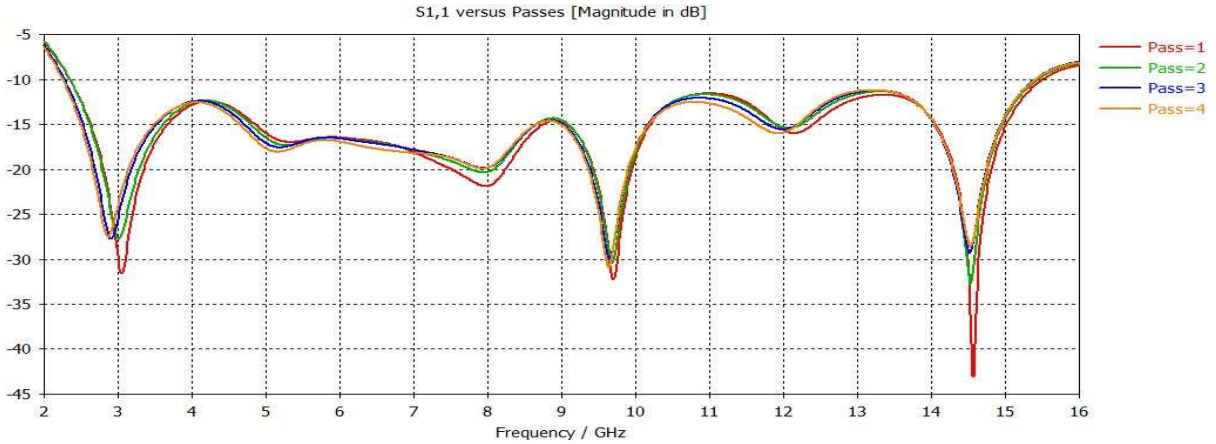

Figure A-1 return loss per pass number for modified antenna.

- **Number of passes frame**

This is the minimum number of passes that will be performed. The mesh adaptation will run for this minimum number of passes, even if the stop criteria are already met. The minimum setting is 2 passes.

This setting determines the maximum number of passes to be performed for the mesh adaptation. The mesh adaptation will stop after this maximum number of passes, even if the stop criteria for the mesh adaptation have not been met. This setting is useful to limit the total calculation time to reasonable amounts [24].

- **Adaptation stop criteria frame:**

Use the change in the S-parameters as stop criterion. The change in the S-parameters has to be below a set threshold (*Maximum delta*) for a number of consecutive passes (*Number of checks*) for the stop criterion to be met.

The change in the S-parameters is determined as the maximal deviation of the absolute value of the complex difference of the S-parameters between two subsequent passes [24].